

IMPROVED CORROSION INSPECTION PROCEDURES FOR REINFORCED CONCRETE BRIDGES: ELECTRICAL RESISTIVITY OF CONCRETE

FINAL PROJECT REPORT

by

O. Burkan Isgor
Oregon State University

Sponsorship
PacTrans and Oregon State University

for

Pacific Northwest Transportation Consortium (PacTrans)
USDOT University Transportation Center for Federal Region 10
University of Washington
More Hall 112, Box 352700
Seattle, WA 98195-2700

In cooperation with US Department of Transportation-Research and Innovative Technology
Administration (RITA)



Disclaimer

The contents of this report reflect the views of the authors, who are responsible for the facts and the accuracy of the information presented herein. This document is disseminated under the sponsorship of the U.S. Department of Transportation's University Transportation Centers Program, in the interest of information exchange. The Pacific Northwest Transportation Consortium, the U.S. Government and matching sponsor assume no liability for the contents or use thereof.

Technical Report Documentation Page

1. Report No.	2. Government Accession No.	3. Recipient's Catalog No.	
4. Title and Subtitle Development of Improved Corrosion Inspection Procedures for Reinforced Concrete Bridges: Electrical Resistivity of Concrete		5. Report Date July 3, 2015	
		6. Performing Organization Code Oregon State University	
7. Author(s) Monica Morales and O. Burkan Isgor		8. Performing Organization Report No.	
9. Performing Organization Name and Address PacTrans Pacific Northwest Transportation Consortium University Transportation Center for Region 10 University of Washington More Hall 112 Seattle, WA 98195-2700		10. Work Unit No. (TRAI5)	
		11. Contract or Grant No. DTRT12-G-UTC10	
12. Sponsoring Organization Name and Address United States of America Department of Transportation Research and Innovative Technology Administration		13. Type of Report and Period Covered Research 7/1/2013-7/31/2015	
		14. Sponsoring Agency Code	
15. Supplementary Notes Report uploaded at www.pacTrans.org			
16. Abstract The effects of steel reinforcement and chloride-induced corrosion initiation on the electrical resistivity measurements using the Wenner probe technique were studied experimentally on custom-designed reinforced concrete slabs. Investigation parameters included (1) probe configurations with respect to rebar mesh, (2) rebar density, (3) epoxy coating on the rebar, (4) concrete cover thickness over embedded reinforcement, (5) chloride ingress, and (6) corrosion of rebar. The concrete moisture condition and cover thickness influenced the effect of rebar mesh. It was theorized that bound chlorides increased electrical resistivity measurements and counteracted the effect of free chlorides. It was observed that epoxy coated rebar did not significantly affect measurements. Uncoated rebar affected resistivity measurements, particularly for saturated and semi-saturated concrete. Corrosion initiation was observed to have no significant effect on measurements. Larger concrete cover thicknesses provided for more discrepancy between half-cell potential and electrical resistivity measurements. Recommendations to increase electrical resistivity measurement accuracy on reinforced concrete slab surfaces are made.			
17. Key Words Concrete; Corrosion; Electrical Resistivity; Wenner Probe		18. Distribution Statement No restrictions.	
19. Security Classification (of this report) Unclassified.	20. Security Classification (of this page) Unclassified.	21. No. of Pages 75	22. Price NA

Table of Contents

Acknowledgments	vi
Abstract	vii
Executive Summary	viii
CHAPTER 1 INTRODUCTION	1
1.1 Background	1
1.2 Objectives and Scope of the Report	4
CHAPTER 2 LITERATURE REVIEW	6
2.1 The Effect of Rebar	6
2.2 The Effect of Cover Cracking	12
2.3 The Relationship between Resistivity and Chloride Transport	17
2.4 The Relationship between Resistivity and Rebar Corrosion	22
CHAPTER 3 EXPERIMENTAL PROGRAM	32
3.1 Materials	32
3.2 Reinforced Concrete Slabs	33
3.3 Testing Program	38
CHAPTER 4 RESULTS AND DISCUSSION	44
4.1 Effects of Rebar, Cover Thickness and Probe Orientation	44
4.2 Effect of Epoxy Coating	47
4.3 The Effect of Chloride Ingress	50
4.4 The Effect of Corrosion Initiation	52
4.5 The Effect of Early Stages of Corrosion	54
CHAPTER 5 CONCLUSIONS AND RECOMMENDATIONS	57
REFERENCES	60

List of Figures

Figure 1.1 Equipotential and current flow lines due to the contact of the Wenner probe to the concrete's surface.....	3
Figure 2.1 Probe configuration with respect to rebar mesh suggested to reduce electrical resistivity measurement error by Salehi et al. [35]	10
Figure 2.2 Normalized resistivity values over the ratio of probe spacing to surface layer thickness containing chlorides [10]	18
Figure 2.3 Reinforced concrete specimen geometry and chloride profile sample selection [46].	20
Figure 2.4 Inverse relationship between corrosion current and concrete resistivity from field measurements [28]	24
Figure 2.5 Suggested methodology when assessing four-point Wenner probe electrical resistivity and half-cell potential measurements [23]	30
Figure 3.1 (a) Experimental design schematic and (b) experimental set up of the uncoated rebar reinforced concrete slab	35
Figure 3.2 (a) Experimental design schematic and (b) experimental set up of the epoxy coated rebar reinforced concrete slab	36
Figure 3.3 Experimental design schematic of the uncoated rebar reinforced concrete slab and measurement locations for (a) during chloride ingress for each Zone and (b) after chloride-induced corrosion initiation for the entire slab after chloride ponding	37
Figure 3.4 Probe configurations with respect to (a) 8-inch spaced rebar mesh, (b) 4-inch spaced rebar mesh	39
Figure 3.5 (a) Experimental schematic and (b) experimental set up of the chloride-inducing corrosion process	42
Figure 4.1 Effect of probe configuration with respect to 4-inch spaced rebar mesh for 3.5-inch, 2.5-inch and 1.5-inch concrete cover thicknesses under (a) dry (b) semi-saturated and (c) saturated concrete moisture conditions	46
Figure 4.2 Effect of probe configuration with respect to 8-inch spaced epoxy coated rebar mesh for 3.5-inch, 2.5-inch and 1.5-inch concrete cover thicknesses under (a) dry (b) semi-saturated and (c) saturated concrete moisture conditions	49
Figure 4.3 The relationship between electrical resistivity over days ponded and half-cell potential over days ponded for Zone 2 within the area including Row 1 and 2 and Columns 2-4.....	51

Figure 4.4 The relationship between electrical resistivity measurements before chloride-induced corrosion and after corrosion initiation for Zone 1, Zone 2 and Zone 3 53

Figure 4.5 Contour maps of (a) half-cell measurements and (b) electrical resistivity measurements using Configuration A for the entire slab after corrosion 55

List of Tables

Table 2.1 Concrete resistivity and risk of corrosion of steel reinforcement [30]	25
Table 2.2: Concrete resistivity and risk of corrosion of steel reinforcement [52]	27
Table 3.1 As-batched material properties for ready-mix concrete.....	33

List of Abbreviations

PacTrans: Pacific Northwest Transportation Consortium

OSU: Oregon State University

RILEM: Reunion Internationale des Laboratoires et Experts des Materiaux

ACI: American Concrete Institute

ASTM: American Society for Testing and Materials

Acknowledgments

This report is produced as part of a larger research project on the investigation of the factors affecting electrical resistivity measurements in concrete structures. The majority of the financial support of this large scale project was provided by Oregon State University. Pactrans funding was used to sponsor a part of this larger research project that specifically focused on the improvement of corrosion inspection procedures for reinforced concrete bridges. Authors express their sincere appreciation to the sponsoring agencies.

Authors would also like to thank Dr. Pouria Ghods and Mustafa Salehi for aiding in the experimental design phase of the project. Technical support of the following graduate students are gratefully acknowledged: David Rodriguez, Tyler Deboodt, Matt Adams, Chang Li and Tengfei Fu. Finally, authors thank the undergraduate research assistants Nathan Jones and Andrew Thomas for their diligent work during all stages of the experimental program.

Executive Summary

In recent years, electrical resistivity of concrete has gained increasing attention as a rapid durability and performance index due to its documented correlation with a number of durability-related parameters such as corrosion rate of steel reinforcement and transport properties of concrete. This report presents part of a larger experimental investigation with the main goal of studying the major factors that affect electrical resistivity measurements using the four-point Wenner technique. These factors include: (1) embedded reinforcement properties (cover depth and rebar spacing); (2) discrete cracking; (3) probe configuration with respect to a crack and rebar mesh; (4) delamination of concrete cover; and (5) chloride-induced corrosion of steel reinforcement. However, this report focuses only on the effect of rebar, and the relationship between electrical resistivity measurements and corrosion of steel reinforcement. The results of the larger experimental investigation that studied the effects of all other factors on electrical resistivity measurements are reported in the thesis of Morales (2015)¹.

The effects of steel reinforcement and chloride-induced corrosion initiation on the electrical resistivity measurements using the Wenner probe technique were studied experimentally on custom-designed reinforced concrete slabs. Experimental results showed that the concrete moisture condition and cover thickness influenced the effect of rebar mesh on electrical resistivity measurements. Uncoated rebar affected resistivity measurements, particularly for saturated and semi-saturated concrete. However, it was observed that epoxy coated rebar did not significantly affect measurements. It was hypothesized that bound chlorides increased electrical resistivity measurements and counteracted the effect of free chlorides. As

¹Morales, M. (2015). "Experimental Investigation of the Effects of Embedded Rebar, Cracks, Chloride Ingress and Corrosion on Electrical Resistivity Measurements of Reinforced Concrete," MS Thesis, Oregon State University, 174 pp.

chloride ingress progressed, electrical resistivity measurements did not necessarily decrease, but rather increased or stayed approximately the same. It is assumed that the bound chlorides may impact electrical resistivity more than free chlorides, in that bound chlorides may be creating for discontinuity within the concrete pore network, counteracting the effect of free chlorides, and increasing electrical resistivity measurements. Crystallization of the bound chlorides may also be aiding in the effect of electrical resistivity of concrete.

Corrosion initiation was observed to have no significant effect on electrical resistivity measurements. Larger concrete cover thicknesses provided for more discrepancy between half-cell potential and electrical resistivity measurements. After corrosion initiation, the correlation between half-cell potential and electrical resistivity values was observed to decrease with increasing cover thickness. This could be due to the larger distance between embedded rebar and the concrete surface, or greater variability within the concrete cover in terms of chloride ingress and bound chlorides.

For future research, it is suggested that measurements are conducted over an epoxy coated rebar reinforced concrete slab with its own unreinforced section in order to identify the effects of epoxy coated rebar, as well as chloride ingress and chloride-induced corrosion for epoxy coated rebar mesh, on electrical resistivity measurements. It is also suggested to conduct chloride profiling for reinforced concrete slab specimens during chloride ponding in order to better quantify the ingress of chlorides and correlate the effect of chloride ingress on electrical resistivity measurements. The effects of advanced levels of corrosion on the electrical resistivity measurements need to be further studied to understand if (1) corrosion affects resistivity measurements in later stages of deterioration, and (2) corrosion can be detected using electrical resistivity measurements.

Chapter 1 Introduction

1.1 Background

Concrete is the most widely used construction material in the world. With its annual production exceeding 10 billion tons globally [1], it is used to construct structures that constitute much of the infrastructure in modern societies. For example, there are over 350,000 reinforced concrete bridges in the United States alone, and average age of these bridges is between 40 and 50 years [2, 3]. In order to manage the issue of ageing infrastructure, State and Federal regulations mandate that these structures are regularly inspected to ensure their safe operation — bridges, for instance, must be inspected one every two years in most jurisdictions. Unfortunately, the large number of reinforced concrete structures and the limited number of qualified inspectors restrict the duration and quality of individual inspections, especially when inspections warrant unwanted traffic disruptions [4, 5]. Therefore, most routine inspections are in the form of rapid visual surveys, which do not generally provide accurate assessments of the durability condition of concrete [6, 7]. The traditional non-destructive testing methods (NDTs) are time consuming, and in most cases, do not assess the durability properties of concrete accurately [4, 8].

In recent years, electrical resistivity of concrete has gained increasing attention as a rapid durability/performance index due to its documented correlation with a number of durability-related parameters such as corrosion rate of steel reinforcement [9-12] and transport properties of concrete [13-17]. The four-point Wenner probe technique is a practical method for measuring the electrical resistivity of concrete from its surface in seconds without the need for coring samples. Typical Wenner probes consist of four linearly aligned probes. The two outer electrodes induce an alternating current (AC) into the concrete, I (mA). The two inner electrodes then measure the

potential difference, ΔV (V), resulting from the induced AC electrical current [4, 18, 19], as illustrated in Figure 1. The resistivity of the concrete, ρ (k Ω -cm), is then calculated via:

$$\rho = 2\pi a \frac{\Delta V}{I} \quad (1.1)$$

where a (cm) is the probe's electrode spacing, to output an electrical resistivity value of the concrete, ρ , expressed in kiloohm-centimeters (k Ω -cm) [4, 18-21]. Typical electrical resistivity values for concrete vary from 1 to 1000 k Ω -cm depending on its composition and moisture content [22-24]. Equation (1.1) assumes homogeneity and isotropy of the medium, semi-infinity of the conductive volume, and that the electrodes have point contact with the medium [19]. To reduce noise and time spent when measuring electrical resistivity of concrete, commercial Wenner probes use frequencies greater than 10 hertz (Hz).

At these higher frequencies, embedded reinforcement provides alternate impressed current paths, because it is more conductive than concrete. Discrete cracks, depending on their electrical conductivity and location, might also alter current paths and impose geometrical restrictions on the semi-infinite domain assumption. Due to the redirection of current pathlines as well as short-circuiting due to rebar, the presence of both cracks and rebar may introduce even greater error to electrical resistivity measurements. Despite their importance, these effects have not been studied in realistically detailed and controlled large-scale experimental studies.

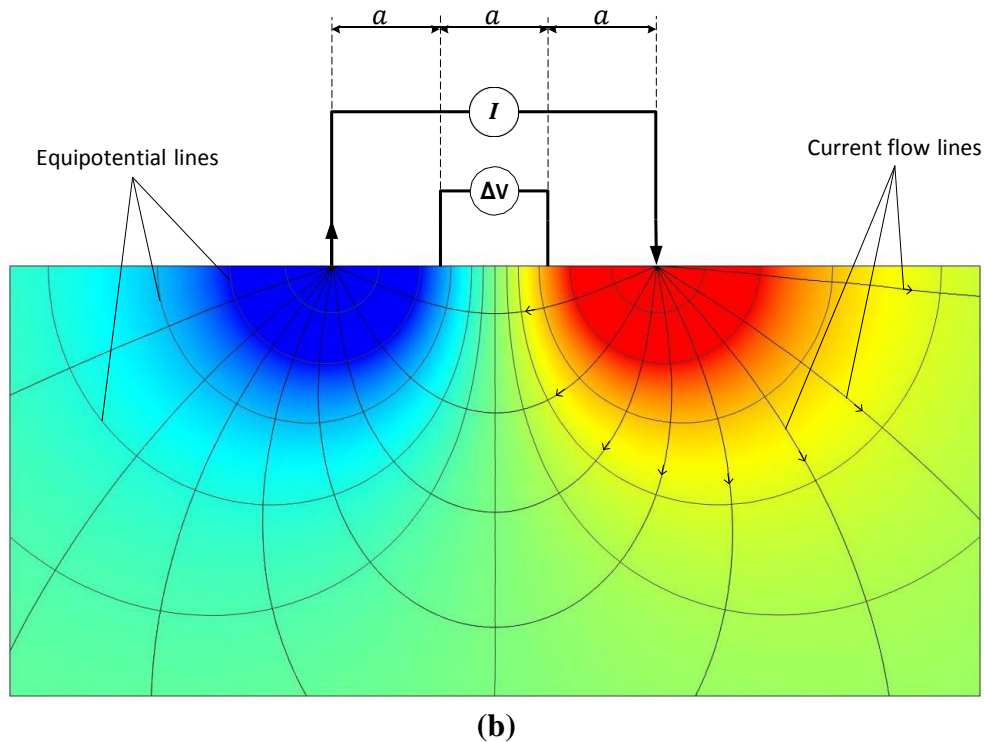


Figure 1.1 Equipotential and current flow lines due to the contact of the Wenner probe to the concrete's surface [25]

One factor that has not been studied so far is the effect of reinforcement corrosion initiation on electrical resistivity measurements using the Wenner probe technique. Corrosion is an electrochemical process that induces electrical currents within the concrete where electrical resistivity measurements are also taken through imposed AC currents. The interaction of these processes might possibly have an effect on the electrical resistivity measurements. As side implication of this would also be that electrical resistivity measurements can be used to detect corrosion initiation if this effect can be demonstrated clearly. In addition, during early stages of corrosion, corrosion products that form on steel reinforcement might change the role of rebar on electrical resistivity measurements: At typical operating frequencies of commercial Wenner

probes, corrosion products on steel might have an insulating effect, diminishing the role of reinforcement on the electrical resistivity measurements. At advanced stages of corrosion, expansive corrosion products might fill concrete pores and cause cracking, altering electrical resistivity measurements. These effects are yet to be studied.

1.2 Objectives and Scope of the Report

This report presents a part of a larger experimental investigation with the main goal of studying the major factors that might affect electrical resistivity measurements using a four-point Wenner probe on a realistically-designed large-scale reinforced concrete slab. These factors include:

- embedded reinforcement properties (cover depth and, rebar spacing);
- discrete cracking (crack type and depth);
- probe configuration with respect to a crack and rebar mesh;
- delamination of concrete cover;
- chloride-induced corrosion of steel reinforcement.

This report focuses only on the relationship between electrical resistivity measurements and corrosion of steel reinforcement. The results of the larger experimental investigation that studies the effects of the other factors on electrical resistivity measurements are reported in the thesis of Moreles [26]. Although these additional aspects of the larger investigation are not presented in this report, a comprehensive literature review is provided.

It should also be noted that the effect of corrosion on electrical resistivity measurements is studied during the early stages of chloride-induced corrosion, specifically, the corrosion currents and initial corrosion products that form on reinforcement. The study of advanced stages of corrosion that manifest, in the form of expansive corrosion products filling concrete pores and

inducing internal cracks, is not part of the current investigation. Moisture and temperature of the concrete is not systematically investigated, but is accounted for when conducting electrical resistivity measurements.

Chapter 2 Literature Review

Electrical resistivity measurements of reinforced concrete structures through the use of a four-point Wenner probe is a practical method to assess the durability of concrete, however, there are many confounding factors that may affect the accuracy of its readings, which are presented in this chapter.

2.1 The Effect of Rebar

Millard [27] and Gower and Millard [28] studied the effect of rebar diameter and spacing, as well as the effect of concrete cover thickness on electrical resistivity measurements using a four-point Wenner probe. Millard's experimental investigation consisted of tanks filled with conductive solution and steel rebar placed parallel to one another within the solution. Probe measurements were taken in between rebar and parallel to rebar at different distances away from the rebar. The main influencing factor was found to be the distance taken away from the rebar, while rebar diameter was not found to be significant in its disturbance. Reduced rebar spacing was found to increase measurement errors. The experimental investigation lacked the use of actual concrete and did not investigate different probe configurations with respect to the rebar or rebar mesh.

Carino [29] provided a summary of the literature for nondestructive test methods when assessing reinforced concrete and stated how reinforcing bars affect electrical resistivity measurements in that the apparent resistivity was lower than the true resistivity value. Carino also restated how concrete cover thickness and the effect of embedded rebar had a strong correlation in that with smaller cover thickness will create for greater error. It was also suggested to take readings midway between two rebar, and suggested that when concrete cover thickness and rebar spacing were small, that a correction factor was possible when the diameter and

location of the reinforcement was known. The correction factor was not explained in detail. No experimental research was conducted, and no recommendations were provided for the presence of rebar mesh.

Weyder and Gehlen [30] studied the effects on Wenner probe electrical resistivity measurements on reinforced concrete blocks in which rebar was spaced parallel to one another. It was found that orienting the probe orthogonally with respect to the embedded rebar, errors on electrical resistivity measurements were reduced. This study lacked the investigation of the effect of rebar mesh and only studied where rebar segments were parallel. It is more common in reinforced concrete structures that rebar is in mesh form spanning both transversely and longitudinally within the concrete, which then may have different influences on measured electrical resistivity than the effect of parallel rebar spanning in only one direction.

Polder's work [31] led to the development of best practices and suggestions for the RILEM TC 154-EMC [32] technical recommendation for taking on-site electrical resistivity measurements. It was stated that errors by a magnitude of two to six-times that of true resistivity can be made from placing all four electrodes over an embedded rebar at 10 or 20 millimeters (0.39 inch or 0.79 inch) depth. It was also warned that if one of the four electrodes was near an embedded rebar, errors will result. Due to the lack of studies on rebar mesh, it was suggested that measurements with a four-point Wenner probe are taken diagonally on the surface of the concrete within the rebar mesh boundary in order to achieve the furthest distance away from the embedded rebar. It was also suggested that five measurements, each a few millimeters in distance from one another, is collected for the area of concern on the surface of the reinforced concrete structure and the median of the five measurements should be stated as the resistivity value for the concrete for that particular area. No recommendations were given for when it is not

possible to fit the probe diagonally within the rebar mesh boundary in the condition where rebar spacing is small. These suggestions were created from summarizing existing literature, however, no experimental work was done in addition to the literature review.

Sengul and Gjorv [33] conducted an experimental investigation to understand the effects of cover thickness, electrode spacing, embedded rebar, probe measurement directions relative to the embedded rebar, and probe measurement distance away from the embedded rebar. Four-point Wenner probes, each with different electrode spacing, were used to conduct the electrical resistivity testing for reinforced concrete test specimens as well as for field measurements on concrete structures. Five different probe configurations with respect to embedded rebar were considered, where four of the five configurations were parallel to rebar, and the fifth was perpendicular to rebar. It was concluded that embedded rebar and electrode spacing affect observed resistivity of concrete. For larger electrode spacing, parallel measurements with respect to embedded rebar significantly reduced observed resistivity, whereas when measurements were made perpendicular to rebar, there were no significant effects to observed resistivity. Sengul and Gjorv [33] suggest that all measurements should be taken as far away as possible from embedded rebar, and if dense reinforcement makes this impossible, electrode spacing should be kept small relative to cover depth. Similar to Gowers and Millar's [10] study, only one rebar was placed within the reinforced concrete block and rebar mesh was not simulated for the laboratory experimental investigation. Rather than sizable reinforced concrete slabs, the measurements were conducted on small specimens which possibly contributed errors to the study due to edge effects.

Presuel-Moreno et al. [34, 35] conducted numerical and experimental investigations involving the effect of the orientation and location of Wenner probe resistivity measurements with respect to embedded rebar. The investigation also involved the effect of the number of

embedded rebar on measurements. This research is an example of the few studies taking into account rebar mesh rather than studying the effect of a single rebar within concrete, as well as the angle of the Wenner probe with respect to rebar (not just parallel and perpendicular configurations). Five different orientations were studied for the presence of rebar mesh, and six different orientation were studied for the presence of a single rebar. From the experimental and numerical results, it was observed that when more than one rebar was present, as in rebar mesh, observed resistivity was significantly reduced. This showed the importance that investigations should be conducted considering rebar mesh when assessing effects on electrical resistivity measurements using a four-point Wenner probe. However, only one rebar mesh density was considered in the study, where smaller rebar to rebar spacing may have different effects on electrical resistivity measurements. Also, most of the probe configurations were investigated within the square created by the four rebar segments. Further investigation in probe configuration with respect to rebar within rebar mesh was not conducted. Different rebar mesh densities and concrete cover thicknesses were also not considered in the study.

Salehi et al. [36] numerically investigated the effect of the presence of rebar mesh in concrete on electrical resistivity measurements conducted with a four-point Wenner probe. The effects of different concrete thicknesses, slab thicknesses, rebar diameter, rebar mesh densities and probe configurations with respect to the rebar mesh were studied. From numerical results, it was found that configuring the probe parallel to the top rebar within the rebar mesh (rebar closest to the concrete surface) and perpendicular to bottommost rebar achieved the smallest error when measuring electrical resistivity of concrete in the presence of rebar mesh. This configuration is represented in Figure 2.1.

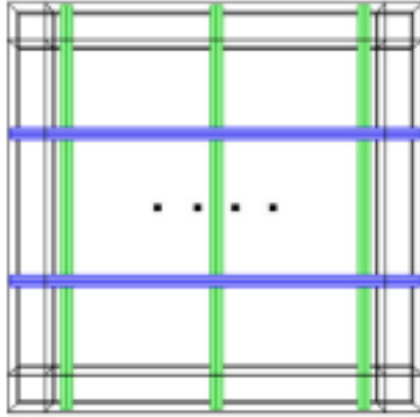


Figure 2.1 Probe configuration with respect to rebar mesh suggested to reduce electrical resistivity measurement error by Salehi et al. [36]

It was also concluded by Salehi et al. [36] that the effect of rebar diameter on electrical resistivity measurements was negligible. As rebar mesh densities increased, it was found that the observed resistivity decreased. There was no experimental investigation to confirm the conclusions based on the numerical study results, but it was one of the few investigations that includes rebar mesh and probe configuration with respect to rebar in its assessment of the effects of reinforcement to electrical resistivity measurements.

Chen et al. [37] experimentally investigated the influences of specimen shape and size, electrode spacing, and cover thickness on electrical resistivity measurements made with a four-point Wenner probe. It was suggested that a correction factor should be applied to resistivity measurements corresponding with the ratio of specimen length to electrode spacing as well as the ratio of specimen diameter to electrode spacing for cylindrical concrete specimens. For prismatic specimens, it was concluded that no correction was necessary with the contingency that the applied current did not pass through the reinforcement. The study did not observe larger specimens or specimens containing more than a single rebar.

Garzon et al. [18] experimentally and numerically investigated the effect of embedded rebar on electrical resistivity measurements using the four-point Wenner method. For the experimental investigation, small scaled cylindrical and prismatic specimens were created using a mortar mixture (sand, water and cement). It was concluded that taking measurements directly above rebar was not advantageous, in that polarization will occur due to a double layer at the steel and concrete interface acting as a resistance-capacitor. Suggestions were made to apply a rebar factor to observed resistivity measurements. However, the experimental study did not include the investigation of a reinforced slab, but only reinforced prismatic and cylindrical specimens. The numerical investigation of a slab with rebar lacked the confirmation of an experimental investigation. The experimental study also used mortar mixture (no coarse aggregate) instead of a concrete mixture for the medium the steel was contained, which is not exactly representative of real-world reinforced concrete structures, and may incorporate more error.

Lim et al. [38] numerically and experimentally studied the effect of rebar on electrical resistivity measurements conducted by a four-point Wenner probe. The numerical model included the parameters: cover depth, rebar diameter, electrode spacing and the resistivity of concrete and reinforcement. The study only investigated one probe configuration which was taken directly above and parallel to a single rebar. Lim et al. proposes a quantitative index in the form of a geometric effect rate. The geometric effect rate is suggested to evaluate the effect of reinforcement geometry and is calculated using a resistivity estimation model. The geometric effect rate ranges from 0 to 1, and attempts to display how reinforcement will affect electrical resistivity measurements on concrete under the same conditions. The experimental investigation was conducted to confirm numerical results and the applicability of the geometric effect rate for

on-site measurements. For the experimental investigation, prismatic mortar specimens containing a single rebar for different concrete cover thicknesses (20 mm, 30 mm and 40 mm) and different rebar diameters (13 mm, 19 mm and 25 mm). To remove the mill scale from the rebar segments, the rebar segments were immersed in a diammonium citrate solutions for two days. The mortar prismatic specimens were cured for 45 days before the first measurements were taken. To control moisture conditions of the specimens and reduce measurement errors, the outside of the specimens was coated with an epoxy resin. To achieve a proper connection, a conductive gel was applied to the four electrodes of the probe. True concrete electrical resistivity was assumed to be the readings for measurements taken directly above the rebar for a cover thickness of 100 mm. It was concluded that the geometric effect rate increased with increasing rebar diameter and increasing electrode spacing, and decreased with increasing concrete cover thickness. Although this numerical investigation was followed by an experimental investigation, the experimental investigation was not realistic. Mortar is not completely representative of concrete. Only a single rebar instead of rebar mesh was considered, as well as a single probe configuration with respect to rebar. Other errors could have derived from the assumption that reinforcement under a 100 mm thick mortar cover did not affect electrical resistivity measurements. These readings were used in place of true concrete resistivity, and may have distorted the observed effects of geometric parameters of reinforcement in concrete. The epoxy coating on the mortar specimens may also have introduced error to electrical resistivity measurements in that a barrier is separating the electrodes from contacting the mortar.

2.2 The Effect of Cover Cracking

Chouteau and Beaulieu [39] numerically modeled electrical resistivity measurements for reinforced concrete structures under the conditions of cracking and delamination. It was found

that electrical resistivity measurements were different from when cracking and delamination were present to when they were not present. This observation led to the conclusion that electrical resistivity could be used to identify delamination at early stages. The electrical resistivity measurements were conducted on reinforced concrete structures using 21 linearly aligned electrodes rather than a four-point Wenner probe setup in order to compare the numerical study to an experimental study. The effect on resistivity measurements were not studied systematically, but was only identified as being dissimilar when cracking was present.

Lataste et al. [40] investigated the ability of electrical resistivity measurements to identify and locate cracks and spalling in concrete. This experiment involved on-site measurements on a reinforced concrete slab with durability concerns as well as electrical resistivity measurements conducted in the laboratory on a cracked reinforced concrete beam. Specific studies were conducted in order to differentiate the influence of the crack characteristics, such as crack depth, crack opening and bridging degree between crack lips, on electrical resistivity measurements which were computed numerically and confirmed experimentally. The electrical resistivity measurements were conducted through the use of four electrodes arranged in a square, rather than linearly as in the Wenner probe arrangement. The square electrode array and instrument setup was to allow for the ability of taking measurements in two perpendicular directions without having to rotate the probe between measurements. In order to change electrical resistivity measurement directions, the use of a switch was involved.

Lataste et al. [40] found that when an insulated crack was present, measurements would either be underestimated or overestimated of true resistivity depending on the direction of the imposed current. When current was imposed parallel to the insulated crack, the observed resistivity was less than true resistivity, and conversely, when current was imposed perpendicular

to the insulated crack, the observed resistivity was greater than true resistivity of the concrete. For a conductive crack, parallel measurements underestimated resistivity, and perpendicular measurements was found to have no significant effect on resistivity measurements. As the depth of the crack increased, it was concluded that the effect on measurements increased. Although various cracks were accounted for within this study, it was assumed that rebar was independent of the crack influence despite width or depth of the crack, which may not be the case for the presence of rebar mesh and a deep, conductive crack. Also, the measurements were conducted with a less common square electrode array rather than the Wenner probe array, which could create for different errors and analysis of crack effects on electrical resistivity measurements. Goueygou et al. [41] compared electrical resistivity to the transmission of ultrasonic surface wave measurements in the ability to detect, characterize and localize induced crack patterns. Cracks were created by bending concrete beam specimens using a three-point bending setup in order to localize one main crack within the concrete. It was concluded that both techniques were able to localize the main crack within specimens. Due to complex crack patterns, the depth of the crack was not estimated; therefore, crack depth was not able to be evaluated by either technique. The electrical resistivity setup was the same square probe used in the Lataste et al. study [40], as previously depicted in Figure 1.8, and not the Wenner probe.

Shah and Ribakov [42] assessed the ability of electrical resistivity measurements conducted with a square probe, as in Figure 1.8, to detect and locate cracks and spalling. Both experimental and numerical studies were conducted. The experimental studies involved laboratory specimens, a set of five cubic concrete specimens, one solid, and the other four defected or flawed with an artificial crack the shape of a penny and parallel to the free surface for varying lengths and depths. Another experimental study involved taking resistivity

measurements on-site using a small area on a 40 year-old reinforced concrete slab where cracking was present. Crack depth and differentiating insulative and conductive cracks were studied numerically. It was concluded that insulative cracks resulted in larger observed resistivity and conductive cracks resulted in lower observed resistivity where certain probe configurations were more sensitive to conductive cracks. For shallow cracks, there was a fair correlation between experimental and numerical data. For on-site experimental data and numerical work, crack depth and opening variations had similar qualitative disturbances on electrical resistivity measurements.

Dunn et al. [43] investigated five nondestructive test methods, one of which was electrical resistivity using a four-point Wenner probe, on nine different reinforced concrete bridge decks. The objective of the experimental investigation was to determine the strengths and weaknesses of each nondestructive test method in assessing causes for deck delamination. Two bridge deck assessments were compared and it was found that for one bridge deck, the primary cause for delamination was corrosion, and for the other bridge deck, the causes for delamination were both corrosion and repeated high deflections. These conclusions were validated by taking concrete core samples from the areas of concern as indicated by the nondestructive test methods. The impact echo test method was indicated as an accurate method in identifying delamination. Although electrical resistivity was referenced as a good indicator of a corrosive environment, there was no specific assessment of the ability of electrical resistivity to identify delamination. Corrosion activity and delamination were within the same regions for one sample bridge deck, but the correlation between electrical resistivity measurements and identifying delamination was not suggested or made. It was suggested that more than one nondestructive technique should be used when assessing probable causes of bridge deck delamination for greater accuracy.

Wiwattanachang and Giao [44] studied the ability of electrical resistivity measurements, using a Wenner array on concrete specimens, in identifying crack direction and depth. Two types of cracks were investigated involving artificial cracks made up of plastic sheets which were inserted into the concrete to simulate insulative cracks, as well as cracks developed by a four-step loading test on the tension face of the concrete beams. Resistivity measurements were corrected for the beam geometry of specimens. Measurements taken where cracks were located for both crack types increased observed resistivity. Crack depth and direction was able to be accurately determined by the mini-electric imaging survey conducted with a Wenner probe. Although insulative cracks were investigated, conductive cracks were not. The purpose of this study was to detect cracks rather than to develop correction factors for observed resistivity when assessing the true resistivity of concrete. Different probe configurations with respect to a crack and its systematic effect on resistivity measurements were not investigated.

Taillet et al. [45] assessed cracks and other discontinuities, such as joints, in massive concrete structures within preexisting boreholes using electrical resistivity. They cautioned against using the experimental investigation towards solid massive concrete bodies such as dams and locks due to limitations of depth into concrete that can be assessed using a technique most common for surface damage assessment. A numerical and experimental investigation was carried out, where the experimental results supported the numerical modeling. This study's objective was to detect cracks rather than to correct for them. It is also noted that a DC current was used rather than an AC current, which may have imposed polarization and affected results unfavorably.

Salehi et al. [46] numerically studied the effect of different types, depths, and widths of cracks on electrical resistivity measurements conducted with a four-point Wenner probe. This

was one of the few studies to incorporate both the presence of cracks and rebar mesh in the investigation. Conductive and insulative crack types were studied, where conductive was assumed to be a crack filled with water, and an insulative crack was assumed to be a crack without bridging and filled with air. The Wenner probe orientation with respect to a crack was also numerically investigated. Measurement errors were found to be a maximum of 200% higher than true resistivity of concrete for the presence of an insulated crack between the two inner, potential difference electrodes. Errors were observed to be lower as crack depth for insulative cracks decreased. For conductive cracks, on the other hand, decreasing crack depth did not noticeably affect electrical resistivity measurements. Measured electrical resistivity was observed to be lower than true resistivity for conductive cracks despite the probe configuration with respect to the crack. For insulative cracks, no clear under or over-measurement was observed. It was observed that when rebar mesh was present, the crack and rebar acted independently of one another, where rebar reduced the measured conductivity of concrete. Although Salehi et al. [46] provided a thorough numerical investigation of the effect of cracks for multiple differences in unreinforced and reinforced concrete, the numerical results were not confirmed with an experimental study.

2.3 The Relationship between Resistivity and Chloride Transport

Gowers and Millard [10] reported that the presence of chloride decreases the electrical resistivity of mortar. Electrode spacing was varied for measurements on a mortar specimen subjected to chloride ingress. It was found that numerical results agreed with the experimental results in that measured resistivity was less than true resistivity for larger electrode spacing when compared to the surface layer thickness. The experimental data and theoretical model results are depicted in Figure 2.2. Although mortar with chlorides in its surface layer was studied, no other

comments were made as to the effect of chloride ingress at different levels within the surface layer. The specimens also were consisted of mortar and not concrete, which may affect electrical resistivity measurement results and analysis [10].

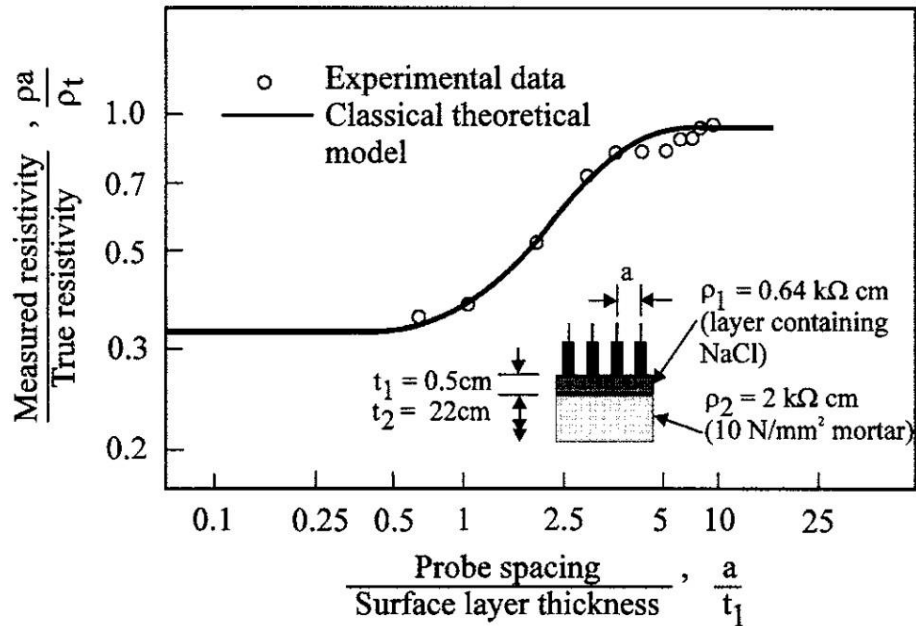


Figure 2.2 Normalized resistivity values over the ratio of probe spacing to surface layer thickness containing chlorides [10]

Polder [31] suggested recommendations and guidelines for on-site electrical resistivity measurements according to the RILEM TC 154-EMC technical recommendation [32] as well as how to interpret those measurements. Chloride penetration was referred to as the initiation period. It was stated that resistivity is inversely related to chloride penetration, where low resistivity equates to areas where chloride ingress will be the quickest in concrete. However, Polder stated that the effect of the penetration of chloride ions on electrical resistivity was relatively small. Polder reviewed the literature and emphasized the inverse relationship between

chloride diffusion rate and concrete resistivity. Although the relationship between electrical resistivity of concrete and chloride ingress was addressed, the effect of chloride ingress on measured resistivity considering different concrete cover thicknesses was not addressed. Polder and Peelen [22] readdressed the inverse relationship between chloride ingress and concrete resistivity determined by previous theoretical and experimental studies. They stated that the chloride diffusion coefficient is also inversely related to concrete resistivity and that low resistivity values will distinguish areas where concrete is more permeable and chloride penetration is higher. It was mentioned again that there is a relatively small effect on electrical resistivity measurements due to the increased chloride content. It was not discussed in detail as to the mechanics behind the effect of chloride ingress at different levels within the concrete cover and no original investigations were conducted to further corroborate the statements on the relationship between electrical resistivity measurements and chloride ingress.

Morris et al. [47] proposed a relationship to be used to predict chloride threshold values from electrical resistivity measurements taken on the concrete surface. The experimental investigation conducted involved sixteen, 15 cm in diameter by 22 cm in height, cylindrical concrete specimens. These specimens contained four rebar segments positioned so that each rebar was protected by a 1.5 cm concrete cover. The reinforced concrete specimen and chloride profile methodology is displayed in Figure 2.3.

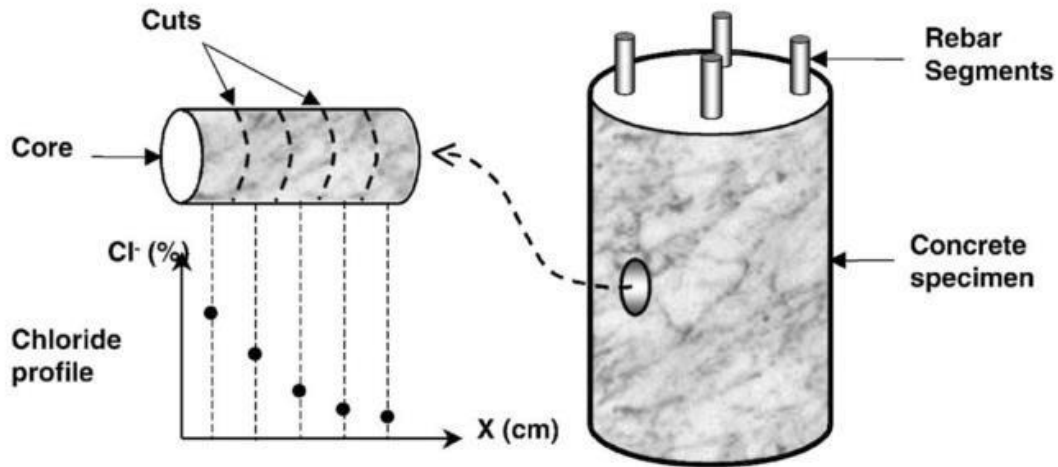


Figure 2.3 Reinforced concrete specimen geometry and chloride profile sample selection [47]

Each cylindrical reinforced concrete specimen was exposed to 1000 days in a marine environment, where half of the specimens were on the seashore and the other half were immersed in seawater. Periodic electrical resistivity measurements were taken over the exposure period. These electrical resistivity measurements were taken on the side of and in between the rebar segments of each cylindrical concrete specimen. Geometrical effects were accounted for when compiling electrical resistivity measurements. It was observed that the rebar was at a passive behavior for resistivity values greater than 30 kΩ-cm, and at a state of corrosion for resistivity values lower than 10 kΩ-cm. The best line of fit for the relationship between chloride content (which was assumed to be the chloride threshold value, Cl_{TH}), in terms of percent chlorides relative to the weight of cement, and resistivity, ρ , in terms of kΩ-cm, was expressed by equation (2.1) [47].

$$Cl_{TH} (\%) = 0.019 \rho + 0.401 \quad (2.1)$$

From the data collected, Morris et al. [47] concluded that resistivity measurements were a good indicator of concrete quality, and that the inverse relationship between chloride ingress and

concrete resistivity stands. Because the study involved cylindrical specimens rather than reinforced concrete slabs where rebar mesh is present, chloride ingress for bridge decks is not closely simulated, and achieving more than one probe configuration with respect to rebar is not possible. Therefore, results from this study may differ for reinforced concrete bridge decks where chloride ingress is sourced from deicing salts and is gravity fed.

Torres-Luque et al. [48] reviewed the literature for the ability, advantages and disadvantages of destructive and nondestructive test methods, including electrical resistivity, to measure chloride ingress in concrete in the laboratory and on-site. Torres-Luque et al. summarized that electrical resistivity is sensitive to chloride presence. It was reviewed that the presence of chloride can increase electrical current and reduce concrete resistivity, and that electrical resistivity measurements could be used to determine chloride diffusion coefficients by estimating chloride profiles. Electrical resistivity using the Wenner probe method was found to be a durable test device in that the embedded parts are manufactured with durable materials such as stainless steel and do not have to be embedded into the structure for testing. Electrical resistivity was not stated to be useful in calculation of the free chloride concentration. Challenges for the development of nondestructive devices were summarized to be the independence of environmental actions such as temperature and moisture condition, the independence of geometry, such as embedded rebar and edges, multi-measurement ability to account for different environmental conditions, and chemical stability, durability and maintainability, as well as cost. Although the literature was reviewed, it was not described in detail how sensitive electrical resistivity is to the presence of chloride ions, or how the transport of chlorides affects measurements.

Andrade et al. [49] introduced a factor to be applied to electrical resistivity measurements conducted with a four-point Wenner probe to account for the retardation of chloride penetration due to the chloride reaction or binding with the cement phases. This chloride penetration retardation factor was presented in order to predict a more accurate diffusion coefficient of concrete. An experimental investigation followed by numerical modelling was conducted. The experimental investigation consisted of cylindrical concrete specimens cured for 28 days, electrical resistivity measurements of the concrete specimens, and subjecting the specimens to chloride ingress to determine diffusion coefficients and if any retardation had occurred. Although the effect on the estimation of the diffusion coefficient was investigated systematically, it was not researched as to how chloride ingress affected electrical resistivity measurements themselves.

2.4 The Relationship between Resistivity and Rebar Corrosion

Although electrical resistivity is an efficient indicator of concrete durability, the only standardized test method for corrosion monitoring is the ASTM C876 half-cell potential mapping technique [50]. Although ASTM C876 provides the probability of corrosion for a certain point on the reinforced concrete structure, it does not provide for the corrosion rate of the reinforcement, which is an important piece of information when gaging the remaining service life span of a structure. If the probability of corrosion is high, but the corrosion rate is very slow, the half-cell potential mapping is concluding a false sense of urgency for repair, when in fact the remaining service life span of the reinforced concrete structure is not being cut short. In the opposite sense, if the corrosion rate is accelerating quickly, but the corrosion probability is read to be low, the half-cell potential testing provides a false indication of the remaining service life span of the structure. Therefore, the appropriate maintenance actions are not taken in order to

resolve the first signs of detrimental corrosion to insure the safety of the public, and provide potential cost savings due to repairs made before corrosion is destructive.

Studies have been corroborating the inverse relationship between corrosive environments in reinforced concrete and electrical resistivity measurements of concrete. As the severity of reinforcement corrosion increases, the electrical resistivity of concrete decreases. However, the effects of the presence of corrosion on electrical resistivity measurements is not thoroughly investigated. Many researchers have stated the relationship of corrosion and electrical resistivity, such as Morris et al. [21] who had mentioned how electrical resistivity of concrete correlates with the possibility of corrosion macrocell currents of the embedded reinforcement.

Carino [29] reviewed the literature and provided an overview of nondestructive techniques, including concrete resistivity, in identifying the status of corrosion in reinforced concrete structures. Concrete resistivity was considered one of the controlling factors for corrosion rate. Thereby, the use of half-cell potential measurements and electrical resistivity measurements in conjunction makes it possible to examine both corrosion probability and corrosion rate. The relationship between concrete corrosion rate and concrete resistivity is shown in Figure 2.4.

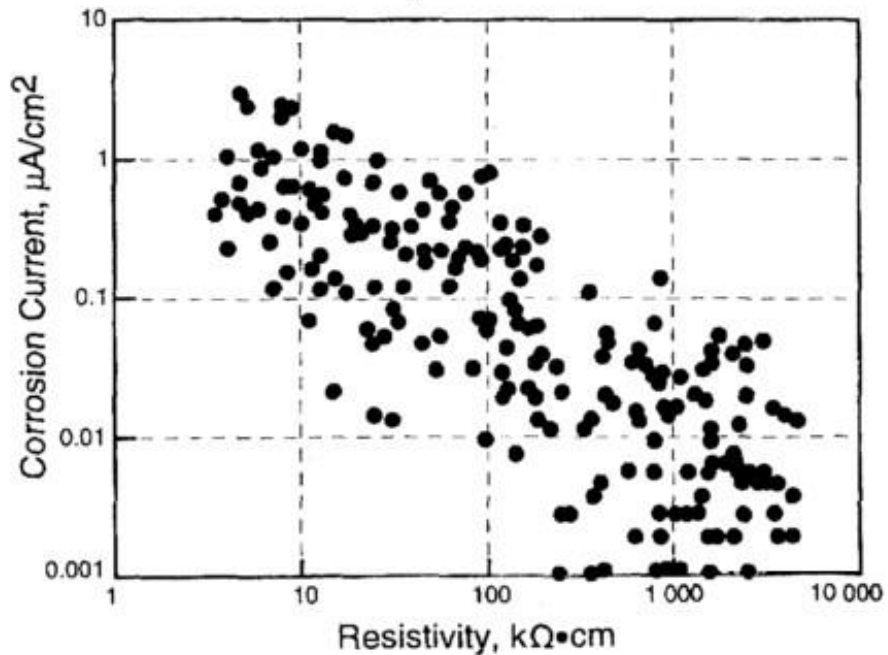


Figure 2.4 Inverse relationship between corrosion current and concrete resistivity from field measurements [29]

It was reviewed that for a high resistivity value, even if the steel is actively corroding as determined by half-cell potential measurements, the corrosion rate may be low; therefore, when steel depassivates, concrete resistivity correlates better with corrosion rate than half-cell potential. Although Carino [29] provided a review of the correlation between resistivity and corrosion, no research was stated to examine the effect of corrosion initiation on electrical resistivity measurements.

Polder [31] also reviewed the literature and provided recommendations for on-site measurements of electrical resistivity on concrete. Contradictory to Carino's [29] review, Polder stated that mapping resistivity measurements did not indicate whether the embedded reinforcement in concrete was actively corroding, and that this information was to be obtained by

using other methods. It was stated that resistivity mapping can show where corrosion was most severe. Polder restated the inverse relationship between corrosion rate of reinforcement after depassivation and concrete resistivity, but this relationship could be different for different concrete compositions. Polder was skeptical of the clear relationship between corrosion rate and concrete resistivity, but provided a general guideline when interpreting electrical resistivity measurements in terms of corrosion risk when applied to ordinary portland cement concrete at 20 degrees Celsius, as seen in Table 2.1.

Table 2.1 Concrete resistivity and risk of corrosion of steel reinforcement [31]

Concrete Resistivity (k Ω -cm)	Risk of Corrosion
<10	High
10-50	Moderate
50-100	Low
>100	Negligible

For values less than 10 k Ω -cm, risk of corrosion was stated to be high, rather than corrosion rate. Although a general rule of thumb was provided for interpreting electrical resistivity values for concrete when assessing corrosion risk, it was not reviewed as to how corrosion initiation itself affects electrical resistivity and the relationship between corrosion rate and electrical resistivity is deemed questionable [31].

Morris et al. [51] evaluated the risk of corrosion of reinforcing steel using electrical resistivity measurement by immersing reinforced concrete specimens in a saline solution.

Corrosion possibilities were identified by half-cell potential measurements. It was suggested that the steel reinforcement is likely to reach a corrosion state when resistivity measurements are lower than 10 k Ω -cm, and reach a passive state when resistivity measurements are higher than 30 k Ω -cm. The corrosion state resistivity confirmed Polder's [31] review, but Morris et al. recorded a lower passivation resistivity value than Polder. Morris et al. confirms that the corrosion rate depended primarily on the concrete quality and initial chloride concentration, and that electrical resistivity is a good indicator of corrosion risk rather than of corrosion rate. Again, the effect of corrosion initiation has on electrical resistivity measurements was not studied and error corrections were not suggested.

Polder and Peelen [22] confirmed the inverse proportionality between corrosion rate and concrete resistivity, and cautions that this relationship is dependent on concrete composition. It was stated that low resistivity values are associated with relatively high corrosion rates after embedded rebar depassivate. Polder and Peelen found that resistivity measurements of concrete reflect its properties in conditions such as chloride ingress, corrosion initiation and corrosion propagation. Corrosion initiation was referred to as the probability of corrosion and corrosion propagation was referred to as corrosion rate. This contradicted Polder's [31] previous study that resistivity is an indicator of corrosion risk and not corrosion rate. Corrosion initiation with respect to electrical resistivity was indicated, but no relationship or effect was developed or elaborated upon.

Gulikers [52] stated how it is very likely that concrete resistivity (specifically of the layer directly near the steel reinforcement rather than the entire concrete cover) plays a decisive role in controlling corrosion rates of embedded reinforcement due to microcell geometric arrangements of anodic and cathodic sites. Guliker also suggested that concrete resistivity does not inherently

control the overall corrosion cell resistance, but rather cathodic activation controls in most cases, whereas in other situations, oxygen diffusion controls where concrete is continuously exposed to wet conditions. Because alternating areas of passively and actively corroding reinforcement will be present in reinforced concrete, the active and passive macrocells will complicate interpretations of half-cell potential and corrosion rate measurements. Gulikers suggested that electrical resistivity may not be the only indication of corrosion rate, but did not review how corrosion initiation may influence electrical resistivity readings and interpretations.

Song and Saraswath [53] reviewed the literature and stated the inverse relationship between concrete resistivity and embedded reinforcement corrosion rate. However, it was found that the evaluation of the degree of rebar corrosion was different amongst researchers. They stated how electrical resistivity was an effective identifier of corrosion risk of reinforcement, especially when corrosion is chloride induced. A table was provided to relate resistivity to corrosion risk in order to assess resistivity measurements as depicted in Table 2.2, which differs significantly from Table 2.1 by Polder [31].

Table 2.2: Concrete resistivity and risk of corrosion of steel reinforcement [53]

Concrete Resistivity (kΩ-cm)	Corrosion Risk
<5	Very High
5-10	High
10-20	Low
>20	Negligible

The relationship between corrosion risk and resistivity Song and Saraswath [53] provided was different from what Polder [31] provided where resistivity values were considerably lower for all corrosion risk levels, and a moderate corrosion risk was not provided. Song and Saraswath [53] suggested that for resistivity values less than 5 k Ω -cm, the corrosion risk is very high, and that for resistivity values greater than 20 k Ω -cm, the corrosion risk is negligible. Corrosion rate and corrosion risk were both referred to within this review, but no clear indication of which resistivity values have a better correlation with was not given. Although relationships between corrosion and resistivity were suggested, how corrosion initiation affects resistivity measurements was not indicated.

Dunn et al. [43] evaluated multiple nondestructive techniques in assessing concrete bridge decks including electrical resistivity. Dunn et al. confirmed that electrical resistivity provides information for the potential for a corrosive environment within areas of reinforced concrete, but did not indicate the relationship between resistivity and corrosion rate of embedded reinforcement or the effect that corrosion initiation may have on electrical resistivity measurements.

Gucunski et al. [4] reviewed the literature on electrical resistivity and other nondestructive techniques for their applications and limitations. The primary application of electrical resistivity was found to characterize corrosive environments within reinforced concrete structures and areas susceptible to chloride ingress, as well as an effective indicator of corrosion activity when paired with half-cell potential measurements. Its limitations were listed that the interpretation of electrical resistivity measurements is challenging in that there are many variables that can affect measurements, such as moisture condition, salt content, etc. How each specific variable affects the overall measurement was difficult to assess. Prewetting of the

concrete surface was also found to be a limitation in that added preparation was needed in order to conduct electrical resistivity measurements; therefore, more time was needed to conduct the measurements.

Along with a review of the literature, Gucunski et al. [4] conducted an experimental investigation to assess rebar corrosion within a concrete bridge deck using three technologies, one of which is electrical resistivity. The evaluation was based on how well the devices were able to differentiate the area constructed with new rebar and the area constructed with corroded rebar. The detection of the degree of rebar corrosion was not assessed but rather corrosion activity, corrosion rate and the determination of a corrosive environment. A limitation was found in evaluating corrosion activity and corrosion rate of epoxy-coated rebar. Measurements were collected, but interpretations of measurements with regard to epoxy-coated rebar were not available. It was stated that electrical resistivity is not affected by epoxy coating within the deck, but no further evidence is provided. It was suggested that electrical resistivity or half-cell potential measurements should be used when evaluating deterioration caused by corrosion due to their low cost, relative speed and simplicity. They report that the advantage that electrical resistivity has over half-cell potential is the lack of the need to obtain an electrical connection to embedded reinforcement, although the information obtained from half-cell potential may be of greater importance to certain agencies. Although corrosion was detected, Gucunski et al. lacks the investigation on the degree of corrosion, which, as they stated, is of interest when assessing corrosion in structures.

Sadowski [23] reviewed the literature and found that there were few papers that determined the probability of corrosion by coupling electrical resistivity and half-cell potential techniques to gain perspective on the degree of reinforcement corrosion in concrete. Sadowski

also noted that it was difficult to find a systematic methodology when assessing corrosion probability. It was suggested that using electrical resistivity conducted with a four-point Wenner probe and half-cell potential techniques, the following methodology should be used when interpreting measurements as seen in Figure 2.5. Although a systematic analysis of results was suggested by Sadowski, no correction factors were suggested for electrical resistivity measurements for corrosion conditions. Only identifying the probability of corrosion was suggested when conducting a corrosion assessment [23].

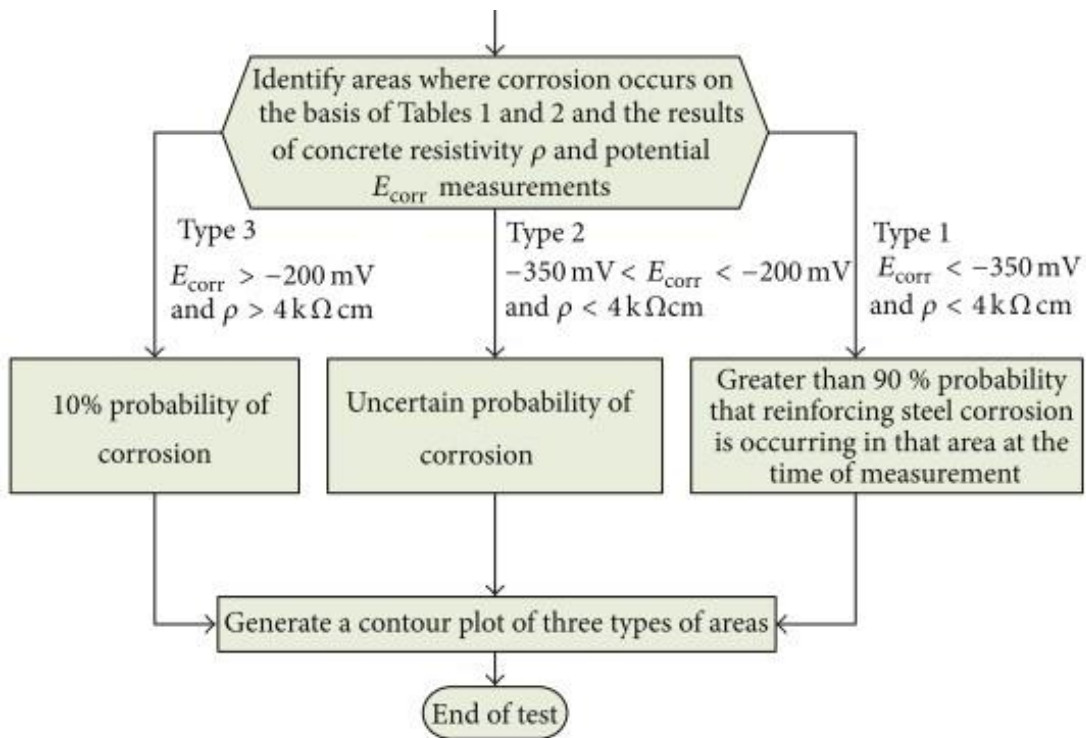


Figure 2.5 Suggested methodology when assessing four-point Wenner probe electrical resistivity and half-cell potential measurements [23]

Hornbostel et al. [54] reviewed the literature for the relationship between corrosion rate of embedded reinforcement and concrete resistivity. They confirm the inverse relationship between concrete resistivity and corrosion rate, not risk. The discrepancies within the literature was summarized and included: (1) the large range and scatter for correlations between corrosion rate and concrete resistivity for resistivity measurements assessments, (2) corrections to corrosion rate measurements may not have been applied, (3) graphical data was not consistent between investigations to show relationships, (4) large scatter of data and few investigations on the effect of moisture state and temperature on the corrosion and resistivity relationship, (4) the lack of investigation of the effect of the cause of corrosion on the corrosion and resistivity relationship, and (5) the lack of knowledge on which mechanism dominates the corrosion process and how this influences resistivity measurements. It was suggested that more field data should be collected and analyzed in order to practically assess the corrosion and resistivity relationship, and that, overall, the relationship between corrosion rate and resistivity should be investigated further.

The relationship between corrosion and electrical resistivity has been experimentally investigated by a number of researchers, as summarized in this section. The electrical resistivity and corrosion relationship is not clear as to if electrical resistivity is correlated with corrosion rate or corrosion risk, but electrical resistivity value ranges were provided in the literature for interpretation of corrosion conditions in reinforced concrete structures, nonetheless. However, after reviewing the literature, the effect that corrosion initiation or corrosion products have on electrical resistivity measurements has yet to be systematically studied by either numerical or experimental investigations.

Chapter 3 Experimental Program

3.1 Materials

The materials for the experimental investigation consisted of ready-mix concrete and rebar, to produce two reinforced concrete slabs in the OSU Outdoor Exposure Site. The design details of the reinforced concrete slabs are provided in the next section. The fresh properties of the commercial ready-mix concrete included an air content of 5.0%, a slump of 5.25 inches and a fresh unit weight of 140.9 lb/yd³. The maximum size aggregate (MSA) for coarse aggregate was ¾-inch. The portland cement (PC) used was a Type I/II and the water-to-cement-ratio (w/cm) is 0.44. The as-batched material contents are provided in Table 3.1.

The natural coarse aggregate and fine aggregate are basalt/andesite based and were excavated in Corvallis, Oregon. The manufactured sand was from cobble which was originally too large to use for portland cement concrete that is broken down to be used as fine aggregate. An air entraining agent (Grace Daravair) and a water reducing agent (Grace WRDA-64) were used during mixing. The concrete was batched, mixed and brought to the outside exposure site by a mixer truck.

The steel reinforcement consisted of uncoated and epoxy coated, size #5, Grade 60 rebar. Placed underneath rebar mesh are six stainless steel plates, three of which are 8-inches by 24-inches and the other three are 16-inches by 24-inches in dimension. Each plate had an electrical connection in the form of two steel wires spot-welded to each plate.

Table 3.1 As-batched material properties for ready-mix concrete

Material	As-Batched
Fine Aggregate Sand (lb/yd ³)	1073
Fine Aggregate Manufactured Sand (lb/yd ³)	203
3/4 inch MSA Coarse Aggregate (lb/yd ³)	1797
Mixing Water (lb/yd ³)	214
Type I/II PC (lb/yd ³)	607
Superplasticizer (fl oz)	24.00
Air Entraining Agent (fl oz)	6.00
w/cm	0.44
Fresh Unit Weight (lb/yd ³)	140.9
Slump (inches)	5.25
Air Content (%)	5.0

3.2 Reinforced Concrete Slabs

Two reinforced concrete slabs were produced for this experimental investigation. One slab was reinforced with uncoated rebar, while the other was reinforced with epoxy coated rebar. The schematic design details of the slabs are shown in Figures 3.1-3.3.

The uncoated rebar reinforced concrete slab was 12-feet wide by 8-feet long and 7.5-inches thick. The slab consisted of three zones with three different concrete cover thicknesses: Zone 1 (3.5-inch cover), Zone 2 (2.5-inch cover), and Zone 3 (1.5-inch cover). Each zone was 4-feet wide and 8-feet long. A 20-inches by 20-inches area was left unreinforced in the corner of Zone 1 so that measurements can be taken without the rebar effect. In each zone, there was an area reinforced with a dense rebar mesh with rebar spacing of 4-inches center to center, as well

as a less dense area with a rebar spacing of 8-inches center to center as shown in Figure 3.1. The rebar mesh of each zone was electrically isolated from the rebar mesh of other zones. Similar to the uncoated rebar reinforced concrete slab, the epoxy rebar reinforced concrete slab also contained three zones with three different concrete cover thicknesses: Zone 1 (3.5-inch cover), Zone 2 (2.5-inch cover), and Zone 3 (1.5-inch cover). Each zone is 32 inches wide by 48 inches long as depicted in Figure 3.2. The epoxy rebar reinforced concrete slab was 8-feet wide, 4-feet long and 7.5-inches thick. Throughout the slab, the density of the reinforcing mesh was the same; i.e., rebar was spaced at 8-inches center to center.

Twelve concrete cylindrical specimens, 4-inches in diameter and 8-inches in height, were cast on the same day the concrete was poured. The reinforced concrete slabs were cured for 21 days using wetted burlap. The other nine cylindrical specimens cured within a moist room according to ASTM C511 [29] for compressive strength testing. At a 28-day concrete age, average compressive strength obtained from nine cylinders was 25.4 MPa (3,680 psi) with a standard deviation of 270 psi.

In order to electrochemically migrate chlorides through the hardened concrete towards the steel rebar within the uncoated reinforced concrete slab to initiate chloride-induced corrosion, six stainless steel plates were bolted to the bottom of the formwork as depicted in Figure 3.1b. Figure 3.3 shows the chloride ponding areas, where a 21% NaCl solution was ponded, the location of the six steel plates, and the measurement locations for each Zone. Theoretically, the steel plate locations were designed to be the locations where corrosion would initiate. However, it is possible for corrosion to happen within the entire ponded area despite the locations of the steel plates, in that chlorides could travel horizontally within the concrete cover.

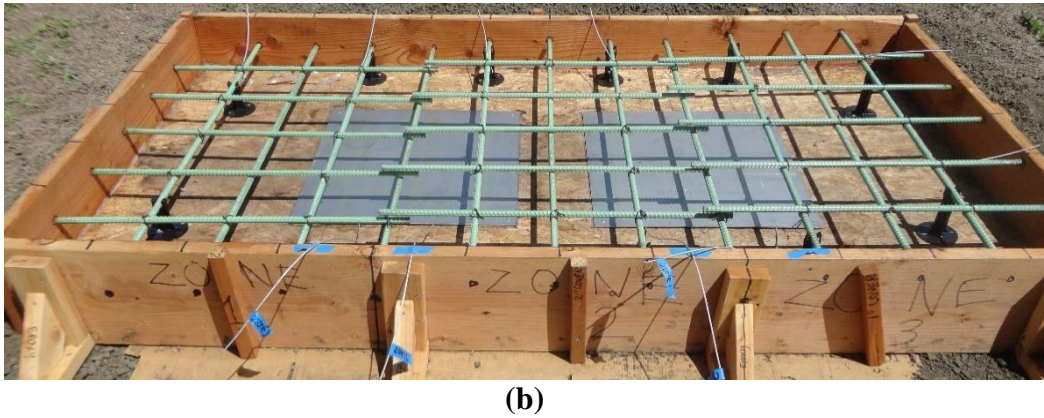
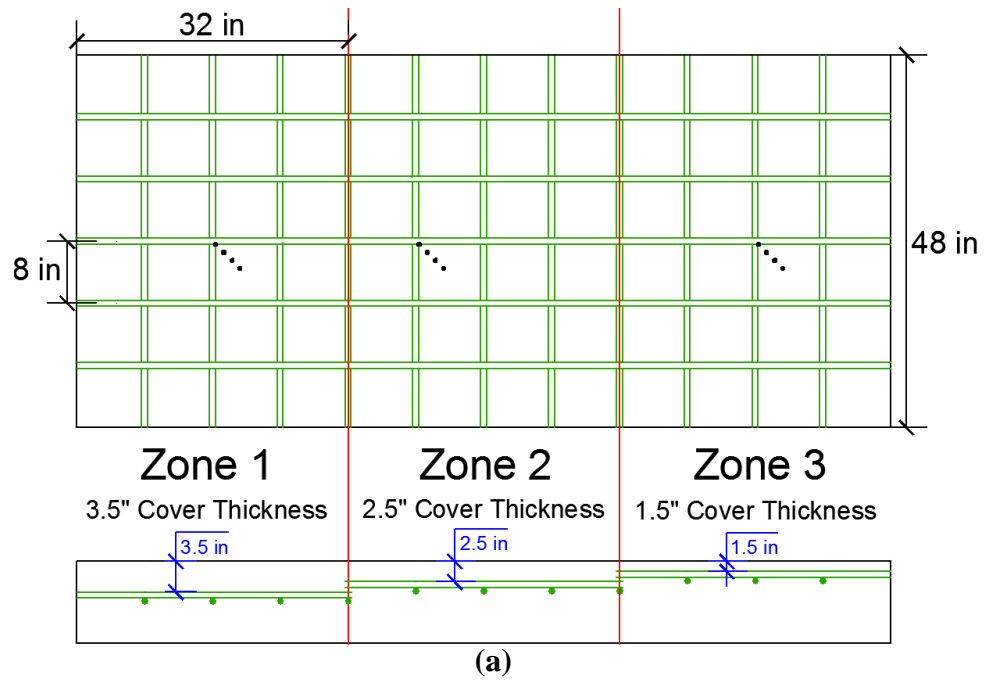
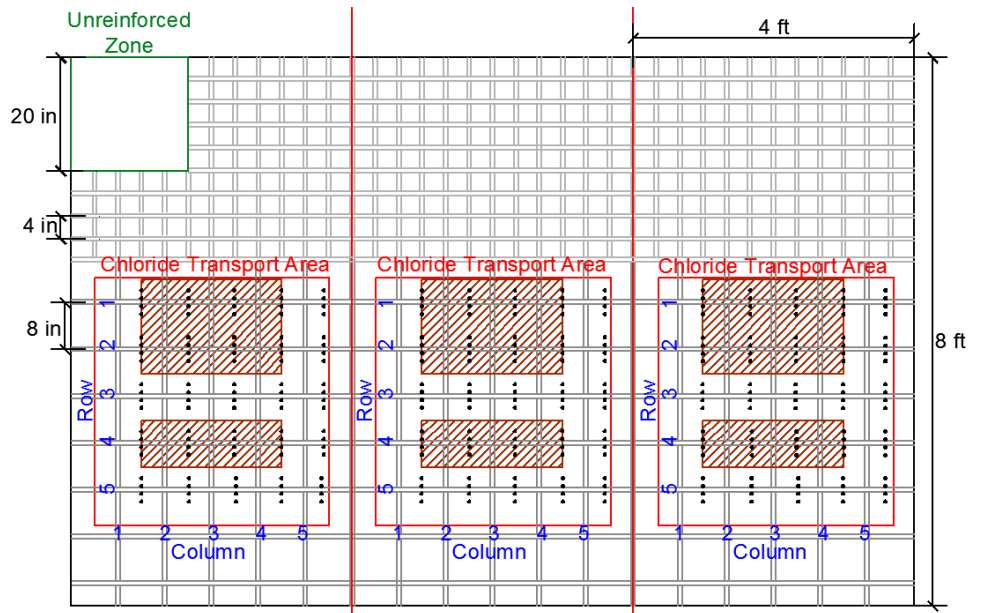
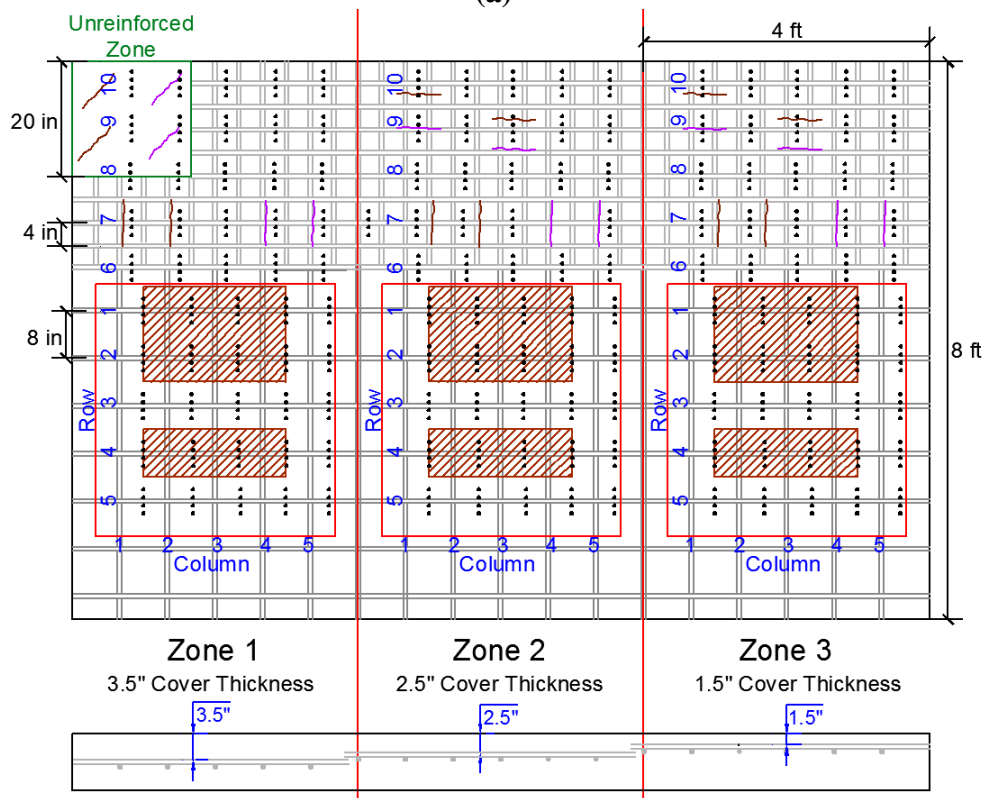


Figure 3.2 (a) Experimental design schematic and (b) experimental set up of the epoxy coated rebar reinforced concrete slab



(a)



(b)

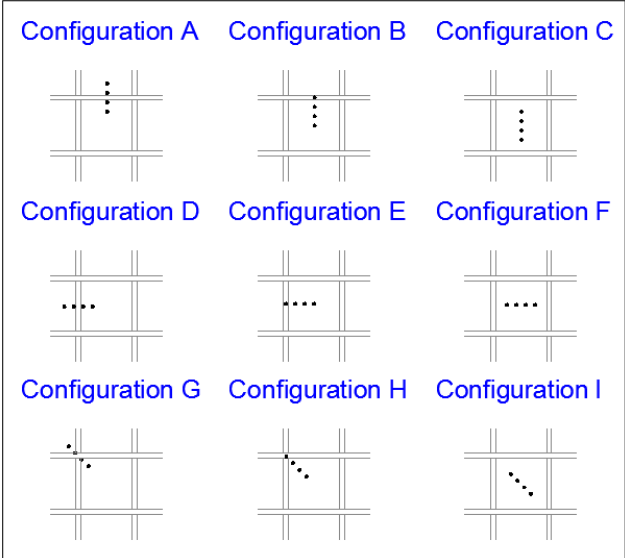
Figure 3.3 Experimental design schematic of the uncoated rebar reinforced concrete slab and measurement locations for (a) during chloride ingress for each Zone and (b) after chloride-induced corrosion initiation for the entire slab after chloride ponding

3.3 Testing Program

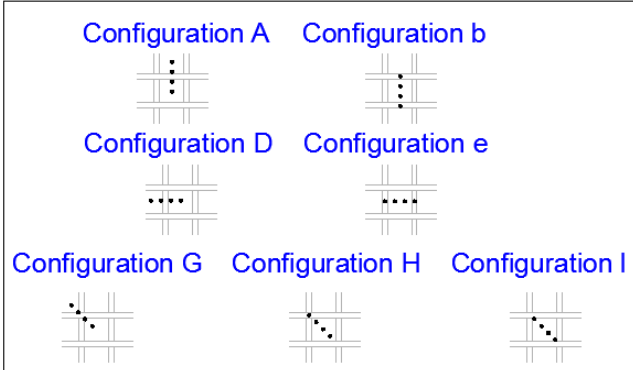
The experimental study involved a testing program that spanned one year starting May 2014 in the Outdoor Exposure Site of the Infrastructural Materials Group at the Oregon State University. After concrete hardened, the use of a rebar locator identified the actual location of embedded rebar for each of the three zones within the reinforced concrete slab and the concrete surface was marked at these locations. These rebar locations were further referenced using markings made on the concrete formwork prior to the concrete pour. Electrical resistivity measurements using a four-point Wenner probe were taken according to the RILEM TC-154 [32] method. Saturated foam caps were used instead of reservoir caps on the probe ends to establish full electrical conductivity between the Wenner probe electrodes and the pre-wetted concrete surface. Probe placements during measurements were facilitated differently for the 4-inch rebar spacing, and 8-inch rebar spacing areas. Probe configurations with respect to the rebar mesh accounted for nine separate configurations for 8-inch spaced rebar mesh, and seven separate configurations for 4-inch spaced rebar mesh [36]. These are shown in greater detail in Figure 3.4.

The median of the five electrical resistivity measurements, for a given location for each configuration, was then normalized by dividing it by the median of five electrical resistivity measurements taken at an unreinforced section of the reinforced concrete slab. If the normalized value is equal to 1, it is to represent true electrical resistivity of the concrete, meaning there were no inflictions to the accuracy of the electrical resistivity reading. Electrical resistivity measurements were taken at a designated area with 4-inch rebar center to center spacing, and at a designated area with 8-inch rebar center to center spacing for each Zone within the uncoated rebar reinforced concrete slab. Electrical resistivity measurements were also taken within each

Zone for the epoxy rebar reinforced concrete slab. Temperature of the concrete surface was also recorded during the time of electrical resistivity data collection using a temperature gun.



(a)



(b)

Figure 3.4 Probe configurations with respect to (a) 8-inch spaced rebar mesh, (b) 4-inch spaced rebar mesh

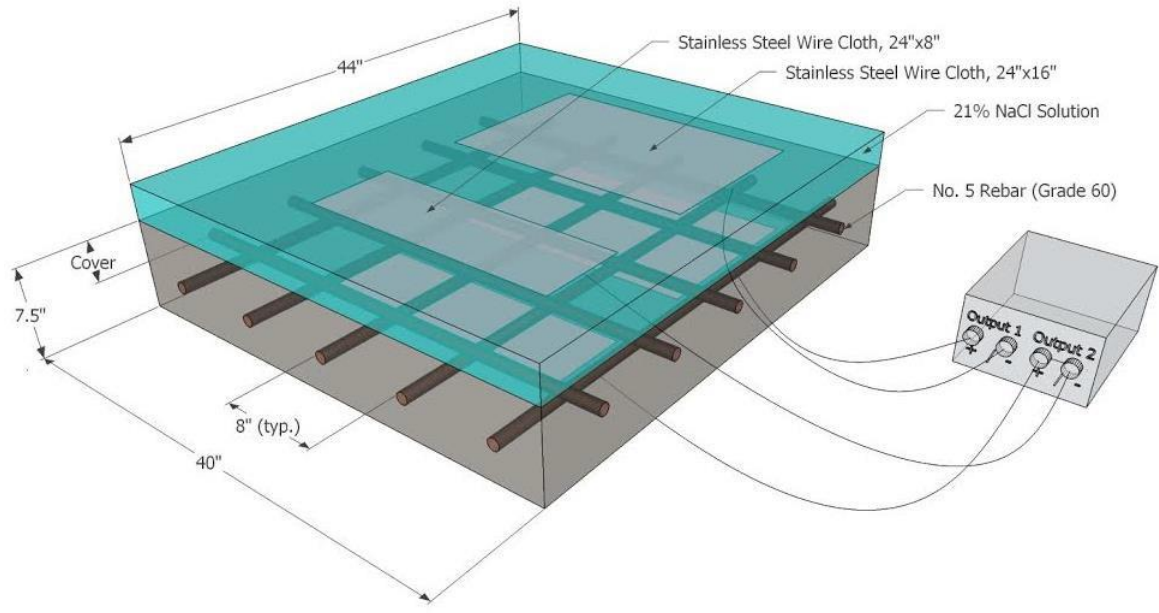
After curing, in order to achieve three different moisture conditions, the reinforced concrete slabs were conditioned for a nearly dry state, a nearly saturated state and a semi-saturated state

(in between nearly dry and nearly saturated). For the dry state, the reinforced concrete slabs endured a week of hot and dry conditions within the exposure site, and the concrete surface was lightly sprayed with tap water in order to collect the electrical resistivity measurements. For the saturated state, the reinforced concrete slabs were ponded using tap water for one week, and electrical resistivity measurements directly followed as soon as the ponds were emptied. The ponds were created by epoxying Styrofoam boards to the sides of the slabs and filled with water, and refilled when the water level lowered, for seven consecutive days. For the semi-saturated state, directly after ponding, the reinforced slabs were left to dry for five days, the sixth day, they endured a rain event, and the seventh day, electrical resistivity measurements were taken.

In order to create chloride-induced corrosion on the steel reinforcement of the uncoated reinforced concrete slab, six steel plates were casted underneath the reinforced concrete slab. Each Zone was ponded separately, beginning with Zone 3 and ending with Zone 1. In order to facilitate ponding, a dam was constructed using Styrofoam boards that were epoxied above the reinforced concrete slab to the concrete surface and filled with 21% NaCl solution created by dissolving generic granular table salt into tap water. A high percentage of NaCl is used in order to simulate high concentrations of chlorides to more rapidly transport chloride into the concrete cover. This chloride transport area is shown by the boxed boundary within the 8-inch spaced rebar mesh in Figure 3.3. Two stainless steel wire cloths, the same dimensions (16-inches by 24-inches and 8-inches by 24-inches) as the stainless steel plates cast to the bottom of the reinforced concrete slab for the three Zones, were placed on the concrete surface directly above the stainless steel plates. A steel wire was spot-welded to each steel plate and steel wire cloth. These steel wire connections were then connected to a Direct Current (DC) power supply. A steel plate at the bottom of the reinforced concrete slab was connected to the positive terminal and the steel wire

cloth on the surface of the reinforced concrete slab was connected to the negative terminal of the DC power supply. With this setup, the steel wire cloth that was submerged in the 21% NaCl solution helped electrochemically migrate chlorides within the solution into the concrete cover towards the embedded steel rebar because of the electrical field created between the steel wire cloth and the steel plate directly underneath it. This chloride-inducing corrosion setup is displayed in Figure 3.5.

Chlorides were able to be relatively quickly transported from the area of high concentration, the salt solution dam, to the area of low concentration, the previously chloride-free concrete towards the embedded steel rebar. The electrical current from the DC power supply was limited to 0.50 amperes for Zone 3, 0.75 amperes for Zone 2 and 1.00 amperes for Zone 3, due to the increase in concrete cover thickness and in order to limit time to corrosion initiation. The DC power supply was removed, and the salt dams were drained at periods before corrosion initiation. The salt residue from the surface of the concrete was cleaned, and the slab was left to be idle for one day before any measurements commenced in order to refrain from effects to measurements due to polarization of the rebar created by the induced current.



(a)



(b)

Figure 3.5 (a) Experimental schematic and (b) experimental set up of the chloride-inducing corrosion process

Measurements consisted of half-cell potential measurements conducted with an Ag/AgCl 0.5M KCl electrode, which is +30 mV versus a copper-copper sulfate electrode (CSE), followed by electrical resistivity measurements conducted by a four-point Wenner probe. The half-cell measurements were conducted according to ASTM C876 [50] where rebar connections were created by drilling out concrete to expose the embedded rebar for each Zone, and drilling a hole into the rebar to insert a steel nail to provide an easy access connection for the voltmeter. The surface of the concrete was wetted prior to taking half-cell potential and electrical resistivity measurements, and temperature readings were taken for each set of half-cell potential and electrical resistivity measurements. Measurements were taken at 25 points for each Zone, at the intersection of bottommost and topmost rebar within rebar mesh as depicted in Figure 3.4. For electrical resistivity measurements, only *Configuration H*, *Configuration I* and *Configuration A* were considered to reduce time spent collecting data and temperature and moisture variations. Again, five measurements per probe configuration were collected, and the median of the five measurements was used to represent the measured electrical resistivity for the probe configuration at one point on the concrete's surface. Measurements were taken throughout the process of chloride ingress for each Zone until corrosion initiation was measured at any point indicated by half-cell potential measurements (-350 mV versus CSE).

Chapter 4 Results and Discussion

Due to the different temperatures the electrical resistivity measurements taken on separate days, it was necessary to create for comparable data sets. Electrical resistivity measurements were normalized by temperature to 25°C using the Hinrichson-Rasch law [55]:

$$\rho_2 = \rho_1 \exp \left[2900 \left(\frac{1}{T_1} - \frac{1}{T_2} \right) \right] \quad (4.1)$$

where ρ_1 is the measured resistivity, ρ_2 is the normalized resistivity, T_1 (K) is the temperature of the concrete during the measurement, and T_2 , is the normalized temperature (i.e., 298.15 K). In addition, most results presented in this section represent a normalized electrical resistivity value, where the measured electrical resistivity value, the median of five measurements, is divided by the actual electrical resistivity value, taken as the median of five electrical resistivity measurements taken within the unreinforced concrete area where it is assumed that rebar has no effect. For values near a ratio of 1.0 for normalized measured resistivity measurements to actual electrical resistivity ($\rho_{\text{measured}}/\rho_{\text{actual}}$), it is assumed that there is no effect on measured resistivity.

4.1 Effects of Rebar, Cover Thickness and Probe Orientation

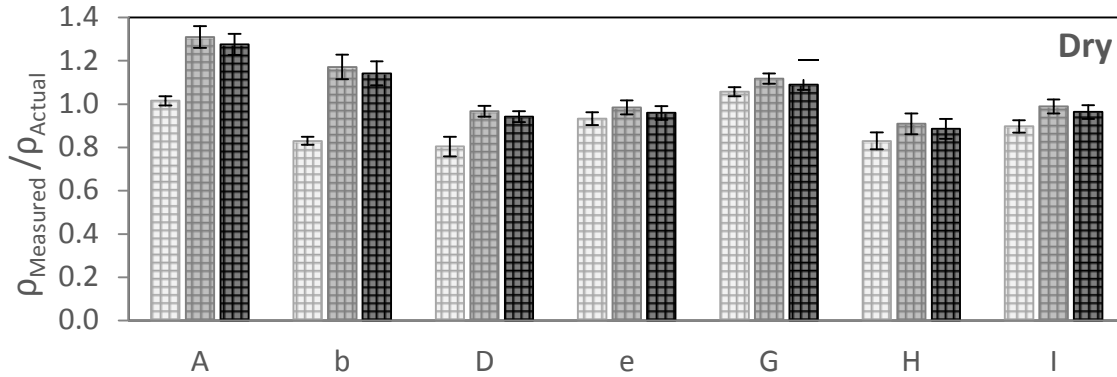
Solely considering one rebar mesh density for all possible probe configurations with respect to rebar mesh, the effect of the probe configuration for each of the three concrete cover thickness can be examined. Figure 4.1 illustrates all probe configurations with respect to rebar mesh considered for 4-inch spaced rebar mesh and 8-inch spaced rebar mesh. Firstly, the effect of probe configurations with respect to 4-inch spaced rebar mesh is shown. Concrete covers of 1.5-inch, 2.5-inch and 3.5-inch thicknesses are displayed, as well as the seven probe configurations considered for 4-inch spaced rebar mesh. The three concrete moisture conditions, dry, semi-saturated, and saturated are displayed separately in separate charts. Again, when values are near a ratio of 1.0 for normalized measured electrical resistivity measurements to actual

electrical resistivity ($\rho_{\text{measured}}/\rho_{\text{actual}}$), it is assumed that there is no effect on measured electrical resistivity. For different concrete moisture conditions, the seven probe configurations with respect to rebar mesh have different effects on electrical resistivity measurements for different concrete cover thicknesses.

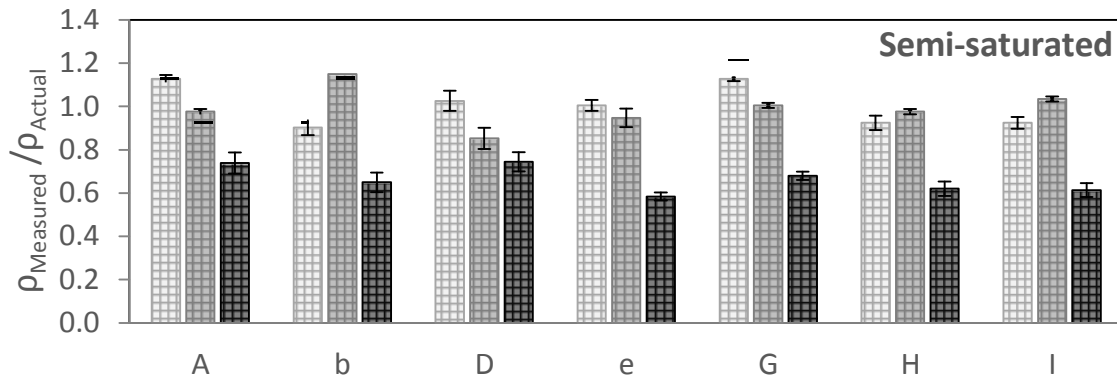
For a dry concrete moisture condition, the probe configuration that provides for the least amount of error over 4-inch spaced rebar mesh are *Configuration e* and *Configuration I* with errors not greater than 7% and 10%, respectively, where the greatest error created for both probe configurations is for measurements over 3.5-inch concrete cover. For measurements over 2.5-inch and 1.5-inch concrete cover, the error is negligible for both configurations (4%).

Configuration e avoids the top rebar layer within the rebar mesh, whereas *Configuration I* tries to avoid the rebar mesh completely. However, contrary to technical recommendations provided by commercial providers [56] for electrical resistivity measurements taken over a more dense rebar mesh, *Configuration A* provides the greatest amount of error (up to 31%) for smaller concrete cover thicknesses.

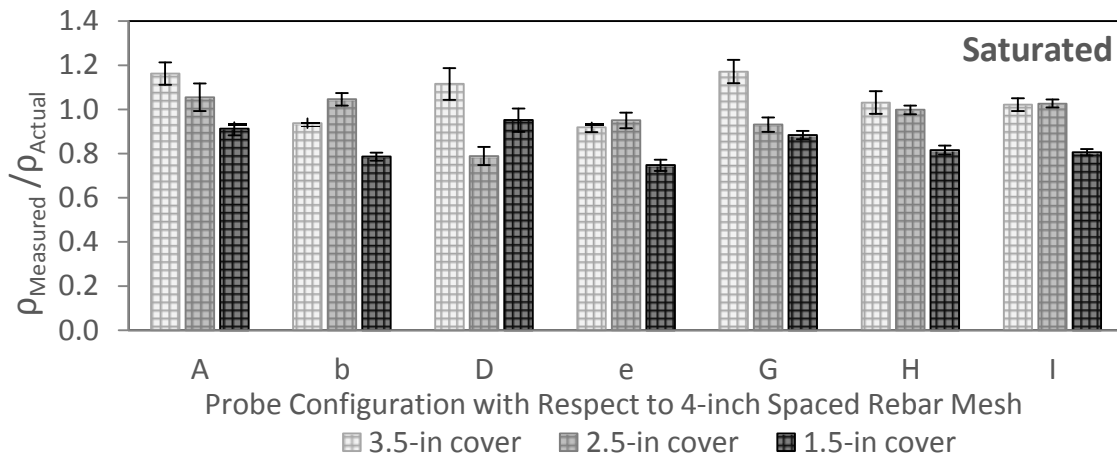
Under a semi-saturated concrete moisture condition for 4-inch spaced rebar mesh, 3.5-inch and 2.5-inch concrete cover thicknesses and all probe configurations do not provide for much error (up to 15%), but for 1.5-inch concrete cover thickness, electrical resistivity measurements are under-measured by 26% to 42% where *Configuration A* provides for the least error. Although probe configuration with respect to rebar mesh does not play a major role in the effect of electrical resistivity measurements for semi-saturated concrete moisture conditions, small concrete cover thickness does. This could be due to the greater connectivity of the concrete pore network by moisture where current is more easily able to be short-circuited by embedded concrete near the concrete surface.



(a)



(b)



(c)

Figure 4.1 Effect of probe configuration with respect to 4-inch spaced rebar mesh for 3.5-inch, 2.5-inch and 1.5-inch concrete cover thicknesses under (a) dry (b) semi-saturated and (c) saturated concrete moisture conditions

For 4-inch spaced rebar mesh within a saturated concrete moisture condition, *Configuration A* provides the least amount of error, up to 16%, for all concrete cover thicknesses investigated. When solely considering 1.5-inch concrete cover for 4-inch spaced rebar mesh in a nearly saturated concrete moisture condition, *Configuration D* provided for the least error of 5%. Again, greater errors are created for measurements taken over 1.5-inch concrete cover, where rebar is more likely to short circuit the induced current provided by the Wenner probe.

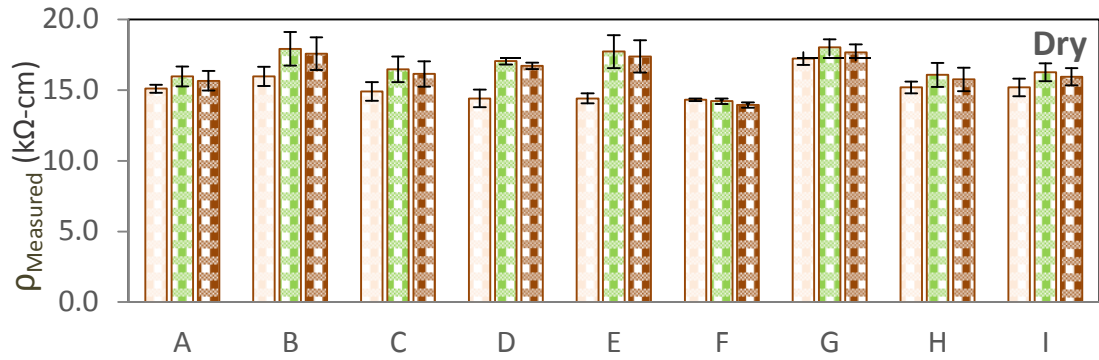
Configuration A, although not superior for dry concrete moisture conditions, provides the best probe configuration and the least overall error for both semi-saturated and saturated moisture conditions for all concrete cover thicknesses. This probe configuration is in accordance to technical recommendations provided by commercial Wenner probe providers [56] when collecting electrical resistivity measurements over a dense rebar mesh. Configuration A for a dry concrete moisture condition may aid short circuiting of the induced current, where embedded rebar provides the path of least resistance within the dry concrete medium, whereas for semi-saturated and saturated moisture conditions, the connected pore-network within the concrete medium may aid the transport of the induced current to bypass the embedded reinforcement.

4.2 Effect of Epoxy Coating

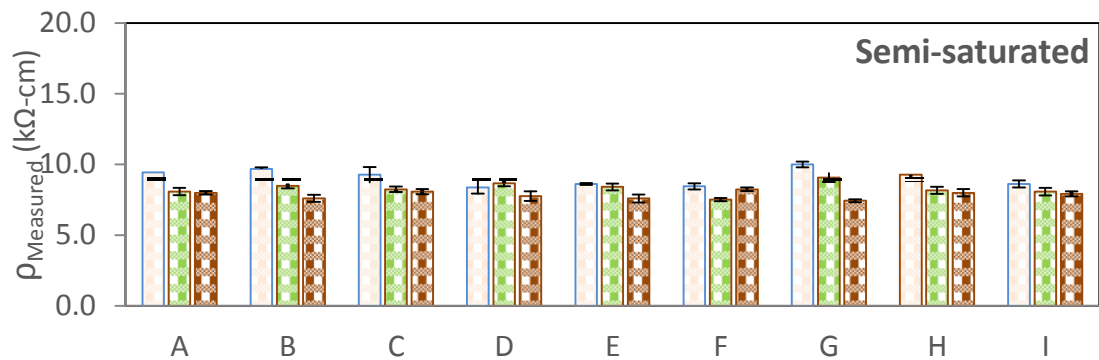
When considering epoxy coated rebar mesh at the same 8-inch spacing, electrical resistivity measurements are less for the epoxy coated rebar concrete slab than for the uncoated rebar concrete slab. The epoxy slab could not be normalized to actual electrical resistivity in that the epoxy slab does not have an unreinforced section of its own. To show how concrete moisture conditions effect epoxy coated reinforced concrete, Figure 4.2 displays the electrical resistivity

measurements (ρ_{measured} in $\text{k}\Omega\text{-cm}$) for dry, semi-saturated and saturated concrete moisture conditions.

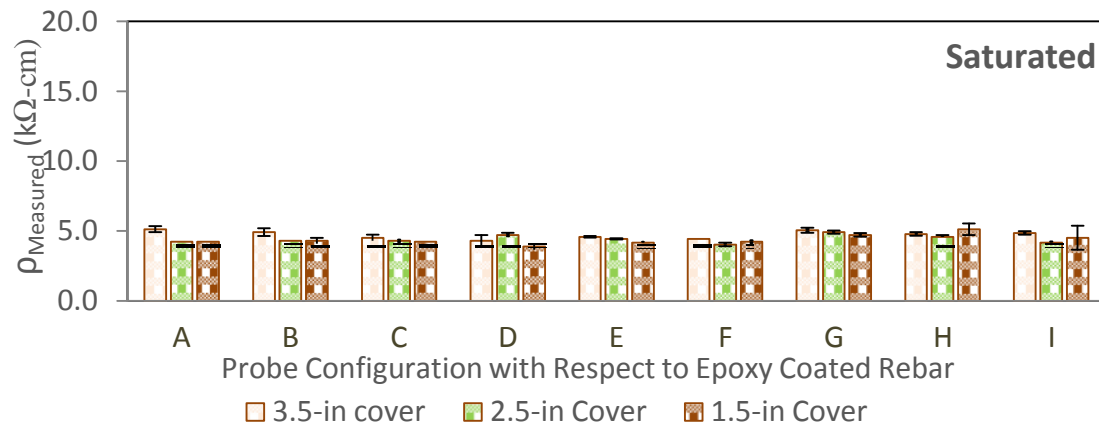
Electrical resistivity measurements are affected nearly the same when considering all probe configurations and all concrete cover thicknesses by epoxy coated rebar mesh for the saturated and semi-saturated concrete moisture conditions. There is more variability due to the effect of probe configuration under dry concrete moisture conditions, but electrical resistivity measurements are still similar. As concrete moisture increases, the measured electrical resistivity decreases, as expected and previously investigated concluded by others. Comparing the dry moisture condition to the saturated moisture condition, electrical resistivity measurements decrease by up to 75% when concrete moisture increases. Probe configuration does not play a role in the effect of electrical resistivity measurements over epoxy coated rebar mesh. Therefore, it is assumed that the epoxy coating does not affect electrical resistivity measurements, however this is not confirmed by normalization to an unreinforced section within the same concrete slab. The epoxy coating may be acting as a barrier between the induced current and the steel rebar and the epoxy layer may impede any short-circuiting of the induced current.



(a)



(b)



(c)

Figure 4.2 Effect of probe configuration with respect to 8-inch spaced epoxy coated rebar mesh for 3.5-inch, 2.5-inch and 1.5-inch concrete cover thicknesses under (a) dry (b) semi-saturated and (c) saturated concrete moisture conditions

4.3 The Effect of Chloride Ingress

Zone 2 containing a 2.5-inch concrete cover thickness, for the surface area enveloping Rows 1 to 5 and Columns 1 to 5 was ponded using 21% NaCl solution for 43 days. For the first 15 days of salt water ponding, electrochemically migrated chlorides were transported into the concrete cover using a current of 0.50 amperes between the surface and bottom of the reinforced concrete slab through the use of the DC power supply. The next 11 days, Zone 2 was ponded with 21% NaCl solution without a current. The following 14 days that Zone 2 was ponded, chlorides were electrochemically migrated into the concrete cover using current at 0.50 amperes until corrosion was initiated. For the last three days after corrosion initiation, Zone 2 was ponded with 21% NaCl solution without a current. Within the 43 days of ponding, ten separate electrical resistivity measurements were taken. Before each measurement was taken, the pond was drained, the surface was cleaned of salts, and was left to sit idle for one day in order to refrain from any polarization effects created by the induced current to the electrical resistivity and half-cell potential measurements.

Figure 4.3 illustrates the relationship between the number of days Zone 2 was ponded with 21% NaCl solution and the value of the electrical resistivity measurements using *Configuration A*, as well as the relationship between days ponded and the value of half-cell potential measurements for the area including Rows 1 and 2 and Columns 2, 3 and 4 (area above the large plate), where the concrete was under the same current and conditions. The median of measurements taken over the six locations underneath the area of constant current is visualized within Figure 4.3. Each electrical resistivity measurement for each point were normalized to temperature and was the median of five measured resistivity measurements taken over that point. The error bars represent one standard deviation.

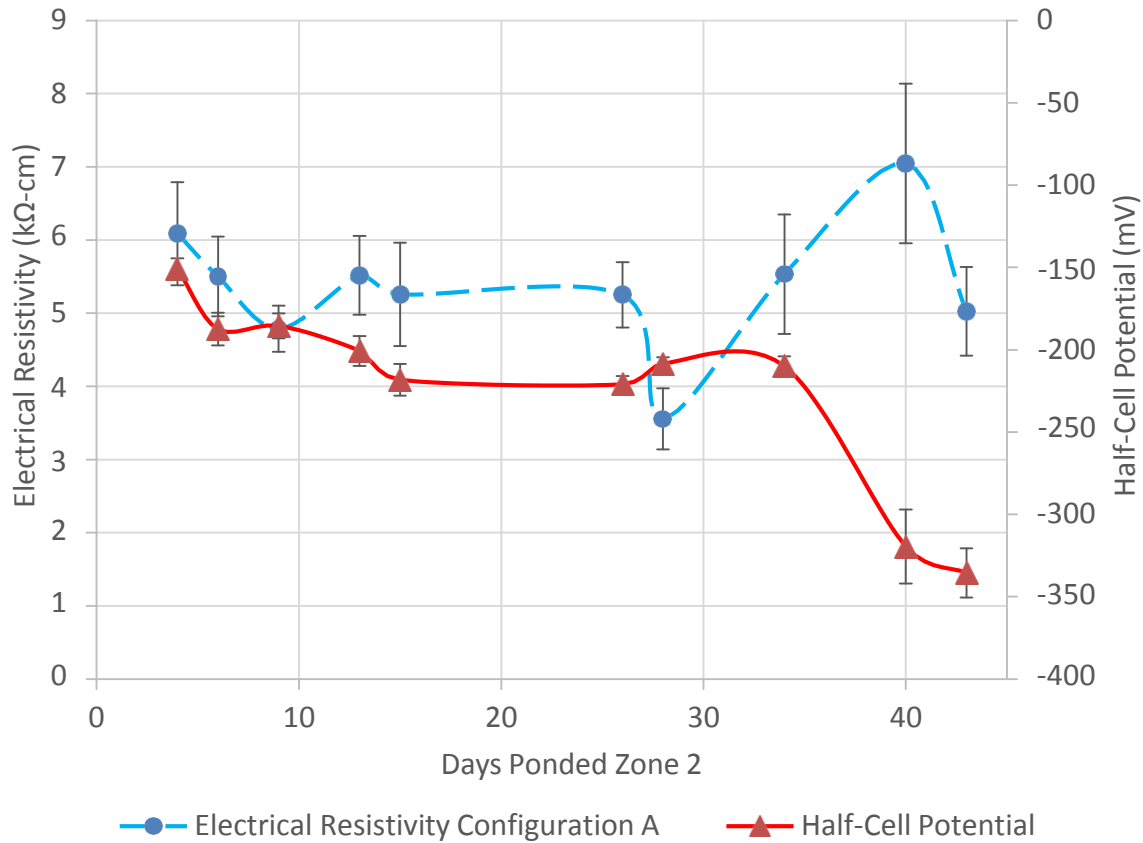


Figure 4.3 The relationship between electrical resistivity over days ponded and half-cell potential over days ponded for Zone 2 within the area including Row 1 and 2 and Columns 2-4

Over the course of the 10 measurements, chloride transported further into the concrete cover and reached the steel in order to initiate corrosion. The ninth measurement (at 40 days ponded) was taken when corrosion initiation was recorded, and the last measurement was taken after corrosion initiation. Although half-cell potential measurements generally became more negative over the course of ponding, especially for the last two measurements, electrical resistivity measurements using *Configuration A*, decrease, do not change, or increase throughout ponding. It is expected that electrical resistivity would decrease with the increase of chlorides in the pore network of concrete, in that ions help create a more conductive electrolyte, however,

from this data set, electrical resistivity does not. One factor that may be contributing to this discrepancy between chloride ingress and electrical resistivity is that free chlorides will help aid the decrease in electrical resistivity, but bound chlorides may not. Free chlorides are chloride ions found within the pore solution, and bound chlorides are bound in the hydrated cement paste within concrete [57]. The bound chlorides may be creating a barrier within the pore network in concrete and creating discontinuity; therefore, bound chlorides may increase the electrical resistivity of concrete by decreasing pathways in the concrete pore network. Also, the bound chlorides may be crystalizing within the concrete as time passes, and further affecting electrical resistivity measurements by adding a different geometrical and resistive effect.

4.4 The Effect of Corrosion Initiation

When considering all three concrete cover thicknesses investigated, electrical resistivity measurements were taken before and until corrosion initiation occurred, as identified with half-cell potential measurements. To understand if corrosion initiation itself has an effect on electrical resistivity measurements, the points within the chloride transport area for each Zone where corrosion initiation was found were investigated. At these points, electrical resistivity measurements using *Configuration A* are compared for measurements taken just before corrosion initiation to measurements taken when corrosion initiation was identified. Figure 4.4 illustrates the relationship between electrical resistivity measurements for before and after corrosion initiation.

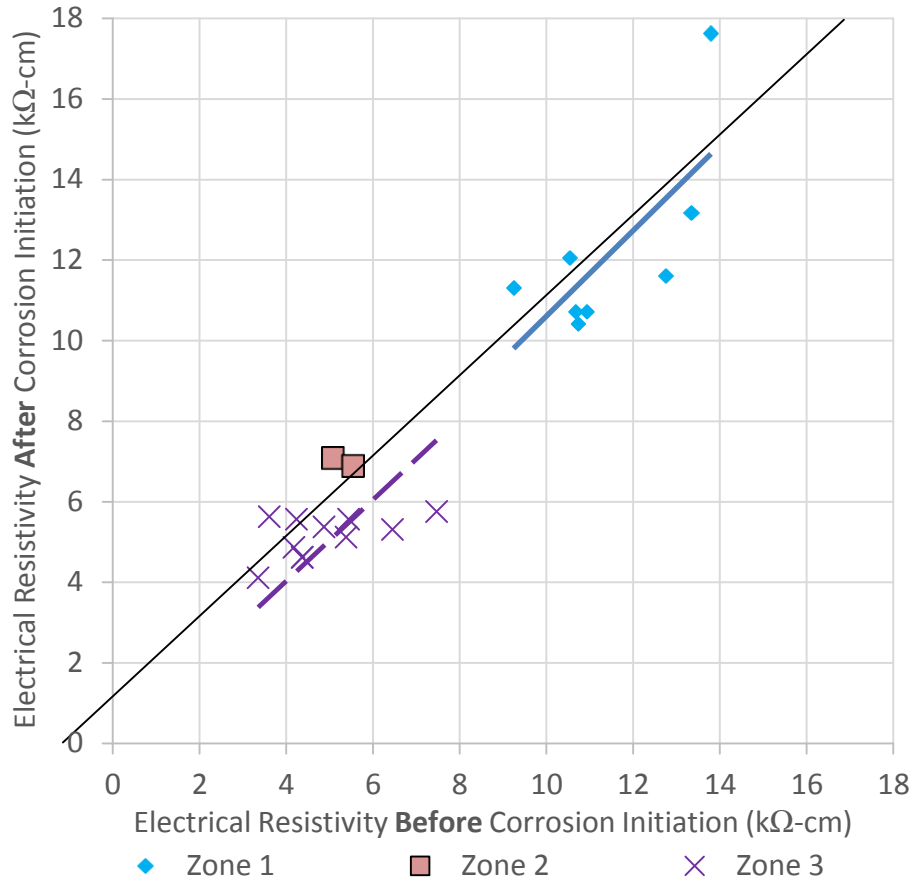


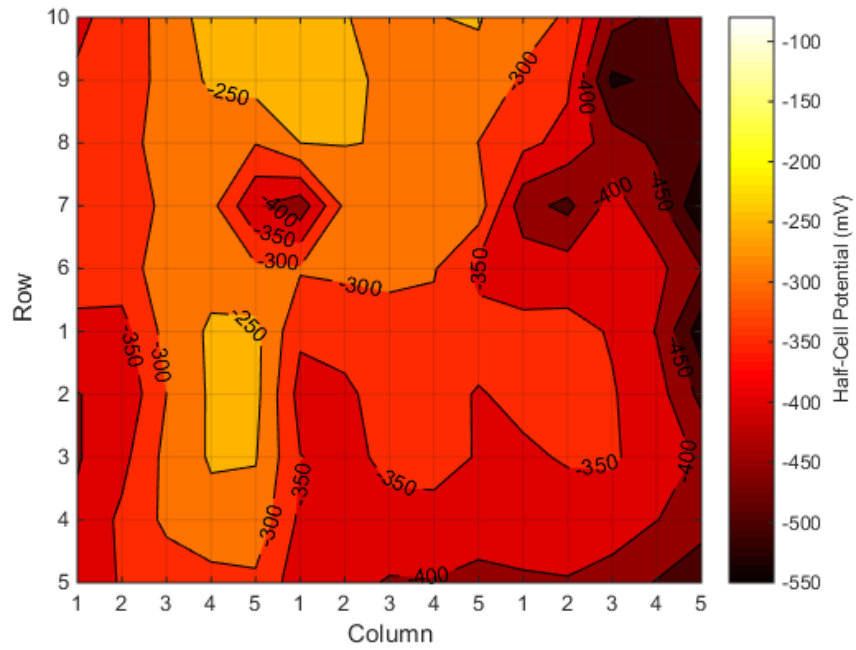
Figure 4.4 The relationship between electrical resistivity measurements before chloride-induced corrosion and after corrosion initiation for Zone 1, Zone 2 and Zone 3

When comparing only the results of electrical resistivity measurements before and after corrosion initiation for Zone 3, the measurements are nearly the same. For Zone 2 and Zone 3, slightly higher values are observed for electrical resistivity measurements taken after corrosion initiation than before corrosion initiation. For small concrete cover thicknesses (i.e. Zone 3), corrosion initiation has nearly no impact on electrical resistivity measurements for this particular reinforced concrete slab specimen investigated, however, as concrete cover thickness increases, corrosion initiation may create for a slight increase in electrical resistivity measurements.

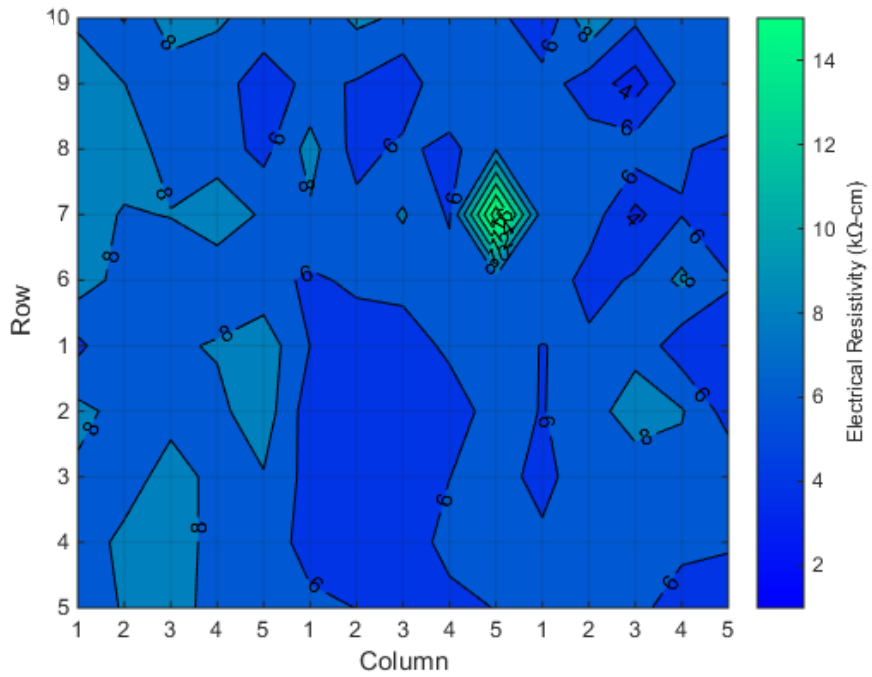
4.5 The Effect of Early Stages of Corrosion

Half-cell potential and electrical resistivity measurements were taken again after corrosion initiation over the entire reinforced concrete slab, after all three Zones endured corrosion initiation, and the areas include the chloride pushing areas, Rows 1 to 5, as well as outside these areas as indicated by Rows 6 to 10. These measurements were conducted directly after the entire slab was ponded with 21% NaCl solution for three consecutive days without an applied current provided by the DC power supply. Figure 4.5 displays the contour maps of half-cell potential and electrical resistivity measurements using *Configuration A* for each of the three zones over the entire slab after chloride-induced corrosion. The three Zones are indicated by Columns 1 to 5 and separated by a thick line. Rows 9 and 10 and Columns 1 and 2, indicate the unreinforced section of the slab and, therefore, are left blank due to lack of reinforcement that may be corroded. As seen in Figure 4.5, low electrical resistivity values generally correspond with low half-cell potential measurements.

At the location Row 7 and Column 5 for Zone 2, a very high electrical resistivity value was obtained. However, this measurement was taken directly above a deep, conductive discrete crack, which created error for the gross over-measurement of electrical resistivity. Electrical resistivity values are generally near or below a value of 8 k Ω -cm for the entire reinforced slab, and are generally near or below 6 k Ω -cm for areas where half-cell potential measurements are most negative. According to ASTM C876, the probability of corrosion is greater than 90% for half-cell potential values less negative than -350 mV [50]. For Zone 3, where concrete cover thickness is smallest, corrosion is probable for approximately its entirety. As concrete cover thickness increases, corrosion probability becomes less due to the greater thickness and, therefore, protection the concrete cover provides for the embedded steel.



(a)



(b)

Figure 4.5 Contour maps of (a) half-cell measurements and (b) electrical resistivity measurements using Configuration A for the entire slab after corrosion

The few major differences between the half-cell potential contour map and electrical resistivity contour map are for locations Rows 3 to 5 and Column 3 for Zone 1, Rows 9 to 10 and Columns 4 and 5 for Zone 1 and Column 1 for Zone 2, and Row 2 and Column 3 for Zone 3. At Row 4 and Column 3 for Zone 1, Row 2 and Column 3 for Zone 3, electrical resistivity values are higher but half-cell potential measurements are very negative. At Row 10 and Column 1 for Zone 2, half-cell potential is less negative, but electrical resistivity is still very low. These opposite values could be due to the corrosion rates of the embedded rebar being faster or slower than the probability of corrosion indicated, the difference of chloride concentration of the concrete cover at those particular locations, or the difference in concrete cover thicknesses. It is observed that there is greater discrepancy for a larger concrete thickness than a smaller concrete cover thickness.

Chapter 5 Conclusions and Recommendations

The effects of steel reinforcement and chloride-induced corrosion initiation on the electrical resistivity measurements using the Wenner probe technique were studied experimentally on custom-designed reinforced concrete slabs. For electrical resistivity measurements conducted over uncoated embedded rebar, for a saturated or semi-saturated moisture condition, *Configuration A* is recommended for either 8-inch spaced or 4-inch spaced rebar, where the greatest error is created for small concrete cover thicknesses and denser rebar mesh (26% for 4-inch spaced rebar under a 1.5-inch concrete cover thickness for a semi-saturated condition). When concrete is at a nearly saturated moisture condition, say, after a long rain event, the greatest errors recorded were 16%; therefore, electrical resistivity measurements are generally more accurate for saturated concrete. It is ideal if electrical resistivity measurements are taken over concrete surfaces after a rain event, and the surface is free of ponding in order to avoid short-circuiting due to standing water.

When taking electrical resistivity measurements on concrete reinforced with epoxy coated rebar, no probe configuration is suggested to achieve the smallest error, in that all configurations investigated create for similar resistivity values for the particular concrete investigated. The most variability is seen for dry concrete moisture conditions; therefore, taking measurements over semi-saturated or saturated concrete is suggested in order to decrease the variability of electrical resistivity measurements.

For a dry concrete moisture condition, it is suggested that electrical resistivity measurements taken over uncoated rebar should be conducted using *Configuration e* or *Configuration I* for 4-inch spaced rebar mesh (greatest error of 10%), and *Configuration C* for 8-inch spaced rebar mesh (greatest error of 4%). When considering the effects of rebar mesh

density and concrete cover thickness on electrical resistivity measurements, the concrete moisture condition plays a major role. For dry concrete with a larger concrete electrical resistivity, it was observed that rebar mesh density and concrete cover thickness do not play a role in affecting electrical resistivity measurements. For semi-saturated concrete moisture conditions, as concrete cover thickness becomes small, rebar mesh becomes of greater influence to electrical resistivity measurements. Within a semi-saturated concrete moisture condition, the 8-inch spaced rebar has nearly the same effect on electrical resistivity measurements as the 4-inch spaced area; therefore, rebar mesh density does not play a role but a small concrete cover thickness does. For saturated concrete, rebar mesh density and concrete cover thickness play a role, where for denser rebar mesh under a small concrete cover thicknesses, electrical resistivity values decrease.

As chloride ingress progressed, electrical resistivity measurements did not solely decrease, but rather increased or stayed approximately the same. It is assumed that the bound chlorides may impact electrical resistivity more than free chlorides, in that bound chlorides may be creating for discontinuity within the concrete pore network, counteracting the effect of free chlorides, and increasing electrical resistivity measurements. Crystallization of the bound chlorides may also be aiding in the effect of electrical resistivity of concrete.

After corrosion initiation, as concrete cover thickness increases, the correlation between half-cell potential and electrical resistivity values was observed to decrease. This could be due to the larger distance between embedded rebar and the concrete surface, or greater variability within the concrete cover in terms of chloride ingress and bound chlorides.

For future research, it is suggested that measurements are conducted over an epoxy coated rebar reinforced concrete slab with its own unreinforced section in order to identify the effects of epoxy coated rebar, as well as chloride ingress and chloride-induced corrosion for epoxy coated rebar mesh, on electrical resistivity measurements. It is also suggested to conduct chloride profiling for reinforced concrete slab specimens during chloride ponding in order to better quantify the ingress of chlorides and correlate the effect of chloride ingress on electrical resistivity measurements. Petrographic analyses on concrete specimens from reinforced concrete containing chlorides over an area where chloride-induced corrosion is identified would also aid in the understanding of the chloride structure within the concrete pore network and its effect on electrical resistivity measurements. The effects of advanced levels of corrosion on the electrical resistivity measurements need to be further studied to understand if (1) corrosion affects resistivity measurements in later stages of deterioration, and (2) corrosion can be detected using electrical resistivity measurements.

References

1. Meyer, C., *The greening of the concrete industry*. Cement and Concrete Composites, 2009. **31**(8): p. 601-605.
2. Mahmoodian, M. and A. Alani, *Time-Dependent Reliability Analysis of Corrosion Affected Structures*, in *Numerical Methods for Reliability and Safety Assessment*. 2015, Springer. p. 459-498.
3. Transportation for America, *One in 9 Bridges Still Structurally Deficient*. 2013.
4. Gucunski, N.I., Arezoo; Romero, Francisco; Zanarian, Soheil; Yuan, Deren; Wigggenhauser, Herbert; Shokouhi, Parisa; Taffe, Alexander; Kutrubes, Doria, *Nondestructive testing to identify concrete bridge deck deterioration*. 2013: Washington, D.C.
5. *ODOT bridge inspection program manual 2013*. 2013, Oregon Department of Transportation. p. 1-381.
6. Zhu, Z., S. German, and I. Brilakis, *Detection of large-scale concrete columns for automated bridge inspection*. Automation in construction, 2010. **19**(8): p. 1047-1055.
7. Moore, W., *Table 1-28: Condition of US Highway Bridges*. National transportation statistics, 2011.
8. Khalim, A.R., et al., *Combination of nondestructive evaluations for reliable assessment of bridge deck*. Facta universitatis - series: Architecture and Civil Engineering, 2011. **9**(1): p. 11-22.
9. Alonso, C., C. Andrade, and J.A. Gonzalez, *Relation between Resistivity and Corrosion Rate of Reinforcements in Carbonated Mortar Made with Several Cement Types*. Cement and Concrete Research, 1988. **18**(5): p. 687-698.
10. Gowers, K.R. and S.G. Millard, *Measurement of concrete resistivity for assessment of corrosion severity of steel using Wenner technique*. Aci Materials Journal, 1999. **96**(5): p. 536-541.
11. Lopez, W. and J.A. Gonzalez, *Influence of the Degree of Pore Saturation on the Resistivity of Concrete and the Corrosion Rate of Steel Reinforcement*. Cement and Concrete Research, 1993. **23**(2): p. 368-376.
12. Morris, W., E.I. Moreno, and A.A. Sagues, *Practical evaluation of resistivity of concrete in test cylinders using a Wenner array probe*. Cement and Concrete Research, 1996. **26**(12): p. 1779-1787.
13. Hamilton, H.R., et al., *Permeability or concrete - comparison of conductivity and diffusion methods*. 2007, University of Florida: Gainesville, FL.
14. Kessler, R.J., R.G. Powers, and M.A. Paredes, *Resistivity measurements of water saturated concrete as an indicator of permeability*, in *NACE Corrosion 2005*. 2005, NACE International: Houston, TX.
15. Millard, S.G., *Reinforced-concrete resistivity measurement techniques*, in *Proceedings of the Institution of Civil Engineers*. 1991. p. 71-88.
16. Polder, R.B. and W.H.A. Peelen, *Characterisation of chloride transport and reinforcement corrosion in concrete under cyclic wetting and drying by electrical resistivity*. Cement & Concrete Composites, 2002. **24**(5): p. 427-435.
17. Sengul, O. and O.E. Gjorv, *Electrical Resistivity Measurements for Quality Control During Concrete Construction*. Aci Materials Journal, 2008. **105**(6): p. 541-547.

18. Garzon, A.J., et al., *Modification of four point method to measure the concrete electrical resistivity in presence of reinforcing bars*. Cement and Concrete Composites, 2014. **53**: p. 249-257.
19. Ueli M. Angst, B.E., *ACI-13-024 On the Applicability of the Wenner Method for Resistivity Measurements of Concrete*. ACI Materials Journal, 2013.
20. Simon, T.K.V., Viktoria, *The Electrical Resistivity of Concrete*. Concrete Structures Annual Technical Journal, 2012. **13**: p. 61-64.
21. Morris, W., E. Moreno, and A. Sagüés, *Practical evaluation of resistivity of concrete in test cylinders using a Wenner array probe*. Cement and Concrete Research, 1996. **26**(12): p. 1779-1787.
22. Polder, R.B. and W.H.A. Peelen, *Characterisation of chloride transport and reinforcement corrosion in concrete under cyclic wetting and drying by electrical resistivity*. Cement and Concrete Composites, 2002. **24**(5): p. 427-435.
23. Sadowski, L., *Methodology for assessing the probability of corrosion in concrete structures on the basis of half-cell potential and concrete resistivity measurements*. ScientificWorldJournal, 2013. **2013**: p. 714501.
24. du Plooy, R., et al., *Development of a multi-ring resistivity cell and multi-electrode resistivity probe for investigation of cover concrete condition*. NDT & E International, 2013. **54**(0): p. 27-36.
25. Salehi, M., et al., *Numerical Investigation of the Effects of Cracking and Embedded Reinforcement on Surface Concrete Resistivity Measurements Using Wenner Probe*. 2013: Carleton University.
26. Morales, M., *Experimental Investigation of the Effects of Embedded Rebar, Cracks, Chloride Ingress and Corrosion on Electrical Resistivity Measurements of Reinforced Concrete*, in *School of Ciivl and Construction Engineering*. 2015, Oregon State University: Corvallis, Oregon, USA. p. 174.
27. Millard, S. *Reinforced Concrete Resistivity Measurement Techniques*. in *ICE Proceedings*. 1991. Thomas Telford.
28. Millard, S., J. Harrison, and K. Gowers, *Practical measurement of concrete resistivity*. British Journal of Non-Destructive Testing, 1991. **33**(2): p. 59-63.
29. Carino, N.J., *Nondestructive techniques to investigate corrosion status in concrete structures*. Journal of performance of constructed facilities, 1999. **13**(3): p. 96-106.
30. Weydert, R. and C. Gehlen, *Electrolytic Resistivity of Cover Concrete: Relevance, Measurement and Interpretation*. Durability of Building Materials and Components 8: Service life and durability of materials and components, 1999. **1**: p. 409.
31. Polder, R.B., *Test methods for on site measurement of resistivity of concrete—a RILEM TC-154 technical recommendation*. Construction and building materials, 2001. **15**(2): p. 125-131.
32. *RILEM TC 154-EMC: Electrochemical techniques for measuring metallic corrosion: Test methods for on-site measurement of resistivity of concrete*. 2000: p. Mater Struct 33(234): 603-611.
33. Sengul, O. and O.E. Gjorv, *Effect of embedded steel on electrical resistivity measurements on concrete structures*. ACI Materials Journal, 2009. **106**(1).
34. Presuel-Moreno, F., Y. Liu, and M. Paredes, *Understanding The Effect Of Rebar Presence And/Or Multilayered Concrete Resistivity On The Apparent Surface Resistivity Measured Via The Four-Point Wenner Method*. 2009, NACE International.

35. Presuel-Moreno, F., Y. Liu, and Y.Y. Wu, *Numerical modeling of the effects of rebar presence and/or multilayered concrete resistivity on the apparent resistivity measured via the Wenner method*. Construction and Building Materials, 2013. **48**: p. 16-25.
36. Salehi, M., P. Ghods, and O.B. Isgor, *Numerical investigation of the role of embedded reinforcement mesh on electrical resistivity measurements of concrete using the Wenner probe technique*. Materials and Structures, 2014: p. 1-16.
37. Chen, C.-T., J.-J. Chang, and W.-c. Yeih, *The effects of specimen parameters on the resistivity of concrete*. Construction and Building Materials, 2014. **71**(0): p. 35-43.
38. Lim, Y.-C., T. Noguchi, and C.-G. Cho, *A quantitative analysis of the geometric effects of reinforcement in concrete resistivity measurement above reinforcement*. Construction and Building Materials, 2015. **83**: p. 189-193.
39. Chouteau, M. and S. Beaulieu. *An Investigation on Application of the Electric Resistivity Tomography Method to Concrete Structures*. in *Geophysics 2002. The 2nd Annual Conference on the Application of Geophysical and NDT Methodologies to Transportation Facilities and Infrastructure*. 2002.
40. Lataste, J., et al., *Electrical resistivity measurement applied to cracking assessment on reinforced concrete structures in civil engineering*. NDT & E International, 2003. **36**(6): p. 383-394.
41. Goueygou, M., O. Abraham, and J.-F. Lataste, *A comparative study of two non-destructive testing methods to assess near-surface mechanical damage in concrete structures*. NDT & E International, 2008. **41**(6): p. 448-456.
42. Shah, A.A. and Y. Ribakov, *Non-destructive measurements of crack assessment and defect detection in concrete structures*. Materials & Design, 2008. **29**(1): p. 61-69.
43. Dunn, M., et al., *Multiple Complementary Nondestructive Evaluation Technologies for Condition Assessment of Concrete Bridge Decks*. Transportation Research Record: Journal of the Transportation Research Board, 2010. **2201**(-1): p. 34-44.
44. Wiwattanachang, N. and P. Giao, *Monitoring crack development in fiber concrete beam by using electrical resistivity imaging*. Journal of Applied Geophysics, 2011. **75**(2): p. 294-304.
45. Taillet, E., et al., *Non-destructive evaluation of cracks in massive concrete using normal dc resistivity logging*. NDT & E International, 2014. **63**(0): p. 11-20.
46. Mustafa Salehi, P.G., O. Burkan Isgor, *Numerical Study on the Effect of Cracking on Surface Resistivity of Plain and Reinforced Concrete Elements*. American Society of Civil Engineers Materials, 2015.
47. Morris, W., A. Vico, and M. Vázquez, *Chloride induced corrosion of reinforcing steel evaluated by concrete resistivity measurements*. Electrochimica Acta, 2004. **49**(25): p. 4447-4453.
48. Torres-Luque, M., et al., *Non-destructive methods for measuring chloride ingress into concrete: State-of-the-art and future challenges*. Construction and Building Materials, 2014. **68**(0): p. 68-81.
49. Andrade, C., R. d'Andrea, and N. Rebolledo, *Chloride ion penetration in concrete: The reaction factor in the electrical resistivity model*. Cement and Concrete Composites, 2014. **47**(0): p. 41-46.
50. ASTM Standard C876 2012, *Standard test method for corrosion potentials of uncoated reinforcing steel in concrete*, A. International, Editor. 2012, ASTM International: West Conshohocken, PA.

51. Morris, W., et al., *Corrosion of reinforcing steel evaluated by means of concrete resistivity measurements*. Corrosion Science, 2002. **44**(1): p. 81-99.
52. Gulikers, J., *Theoretical considerations on the supposed linear relationship between concrete resistivity and corrosion rate of steel reinforcement*. Materials and Corrosion, 2005. **56**(6): p. 393-403.
53. Song, H.-W. and V. Saraswathy, *Corrosion Monitoring of Reinforced Concrete Structures-A*. Int. J. Electrochem. Sci, 2007. **2**: p. 1-28.
54. Hornbostel, K., C.K. Larsen, and M.R. Geiker, *Relationship between concrete resistivity and corrosion rate—a literature review*. Cement and Concrete Composites, 2013. **39**: p. 60-72.
55. Hope, B.B. and A.K. Ip, *Chloride corrosion threshold in concrete*. ACI Materials Journal, 1987. **84**(4).
56. Proceq, S., *Resipod operating instructions*. Schewerzenbach, Switzerland, 2011. **31**.
57. Yuan, Q., et al., *Chloride binding of cement-based materials subjected to external chloride environment—a review*. Construction and Building Materials, 2009. **23**(1): p. 1-13.